Mechanical, thermal, hygroscopic and acoustic properties of bio-aggregates – lime and alkali - activated insulating composite materials: A review of current status and prospects for miscanthus as an innovative resource in the South West of England.

Fabrice Ntimugura [a, *], Raffaele Vinai [a, *], Anna Harper [a], Pete Walker [b]

[a] College of Engineering, Mathematics and Physical Sciences, University of Exeter, Exeter EX4 4QF, UK

[b] BRE Centre for Innovative Construction Materials, Department of Architecture and Civil Engineering, University of Bath, Bath BA2 7AY, UK

*Corresponding authors: fn246@exter.ac.uk (F. Ntimugura) and r.vinai@exeter.ac.uk (R. Vinai)

Highlights:

- Chemical and physical properties of bio-based building materials are presented and analysed
- Interaction mechanisms and their influence on the properties of the composites are examined
- Mechanical and thermal properties as a function of mix designs are summarised
- Acoustic performance of the bio-based materials is reviewed

Abstract

Bio-based building materials are composites of vegetal particles embedded in an organic or mineral matrix. Their multi-scale porous structure confers to them interesting thermal, hygroscopic and acoustic properties. These performance properties have spurred research on these materials as alternative building materials with low embodied energy. This review contains a comprehensive critical analysis of mechanical, thermal, and acoustic properties of bio-based building materials with a particular focus on the interactions of various constituents and manufacturing parameters. Alkali-activated binders are reviewed for their potential use in high strength bio-based composites. A detailed physico-chemical characterisation of the aggregates and compatibility analysis allow a comprehensive understanding of fundamental phenomena affecting mechanical, thermal, and acoustic properties of bio-based building materials. A wide range of biomass materials is available for building composites, and hemp shives remain the most prevalent bio-aggregate. In the context of England, the farming of industrial hemp remains limited, due in part to the long, costly licencing process and the abandonment of processing subsidy as part of the EU common agricultural policy in 2013. On the other hand, Miscanthus (elephant grass) is a perennial, low-energy, and well-established crop in the England which is gaining interest from farmers in the South West region. Its development aligns with actual agricultural, land management and environmental policies with potential to fuel innovative industrial applications. This review performs a critical assessment of

the performance of bio-based materials in an attempt to identify potential frameworks and opportunities to develop building insulating materials from miscanthus.

Keywords: Bio-based materials; mechanical; thermal; acoustic; miscanthus; hemp concrete

1. Introduction

The production of conventional building materials (bricks and concrete blocks) and insulation materials (rock wool, glass wool, extruded polystyrene) consumes substantial energy resources and in return contributes largely to greenhouse gases emissions. The actual environmental challenges and the great contribution of buildings to environmental degradation and resources depletion on one hand, and the increasing energy performance targets for dwellings and other buildings as well as the national and international commitments on CO_2 emission cuts on the other hand, have contributed to channelling research and industrial interests towards low-carbon / bio-based and energy-efficient materials with low embodied energy [1,2]. A successful attempt has been the use of bio-based particles and fibres in combination with mineral binder matrices. Bio-based materials have a triple advantage over traditional materials considering their thermal, hygroscopic and acoustic performances suitable for building envelopes in additional to proven durability and fire resistance [3,4].

Although plant particles-based materials have various sources, hemp shiv has been explored since 1990's. Substantial amount of literature has been published on mechanical, hygroscopic, thermal and acoustic characterization of bio-based building materials [5,6]. Subsequent studies were conducted for in-depth understanding of chemical and physical interactions between components to optimise the performance properties of these materials. The latter include particle-matrix interface-oriented design [7,8], mechanical optimisation through mix design [9] and mix design in combination with manufacturing techniques optimisation [10]. The hygrothermal behaviour of hemp-lime composites was investigated in [11–14] and more recently, the hygrothermal behaviour of hemp-based insulation materials in the UK context was assessed [15].

Mechanical, thermal, and acoustic properties of bio-based building materials (BBBMs) are the basic and benchmarking assets for BBBMs against petrochemical-derived insulating materials. A range of BBBMs exist considering mix designs, envisioned use, and manufacturing techniques. Considering the particularly high porosity of bio-aggregates (59.4 – 78.6% inter particle porosity), interesting thermal performance has been reported to confirm the effectiveness of BBBMs as insulating materials [6,7,9,10]. Literature covering these materials has been recently been published by Chabannes [16] and Amziane [17]. There is an extensive range of BBBMs depending on mix design (binder to aggregate ratio, water to binder ratio), binder nature (lime-based, cement, pozzolanic materials, alkali-activated materials) and other production parameters (aggregates mineralization, compaction, projection, etc.). The transversal analysis of basic properties of these materials is often delicate due to the variety of parameters and samples manufacturing techniques [18].

The objective of this paper is to conduct a critical analysis and summarise mechanical, thermal, and acoustic properties of BBBMs with hemp and miscanthus particles for a comprehensive understanding of the behaviour of these materials. There is a considerable acquired experience on hemp-lime composites over 30 years of research, mainly in France. Furthermore, a recent review summarises factors that influence the performance of hemp concrete [19]. This currently available substantial literature is used to evaluate the potential of miscanthus as an alternative biomass aggregate in the context of the South West England. This paper provides complementary literature data analysis while emphasizing on crucial aspects of microstructural interactions of binders and vegetal aggregates. In addition, alkali-activated binders are explored as potential green binders for BBBMs from the micro-structural point of view. There is an established experience of growing miscanthus, and the potential of reclaiming contaminated mining sites for a further development remains a plausible option in this region. This review covers the chemical composition of bio-aggregates, their physical and chemical interactions with matrices of mineral binders (compatibility) and existing techniques to improve the microstructure and performances of the bio-aggregates composites are presented. In parallel with the literature of chemical behaviour and microstructure, a synthetized and concise presentation of mechanical behaviour, hygroscopic, thermal, and acoustic properties of BBBMs has been made. Finally, the paper discusses environmental motives of developing bio-based building materials and the potential of miscanthus – bio-aggregates in the regional context of South West England.

2. Lignocellulosic materials: physico–chemical properties and mineral matrix interactions mechanisms

2.1. Chemical, physical and microstructural properties of lignocellulosic particle aggregates / fibres.

Contrary to relatively inert mineral aggregates used in concrete; bio-aggregates are chemically sensitive to alkaline aqueous environments. The organic compounds they are made of, dissolve in water, alkaline and acid environments to interact with mineral binders. Their chemical compositions vary from species to species and strongly influence the setting and hardening chemistry of mineral binders. Hemp and miscanthus are non-woody lignocellulosic materials primarily made of cellulose, hemicellulose and lignin, and hence would be subject to interactions when in contact with mineral binders.

2.1.1 Chemical composition of non-wood lignocellulosic materials

Lignocellulosic aggregates and fibres are composed primarily of carbohydrate polymers (cellulose and hemicellulose) and aromatic polymers (lignin), representing at least 70% of the biomass [7]. Advanced chemical analysis of wood and non-wood aggregates and fibres reveals four components: cellulose, hemicellulose, lignin, and extractives (pectins, waxes and fats) in proportions that vary depending on the species and across plant parts. Cellulose occurs in the form of long and slender polysaccharide polymer filaments that develop within the cell walls. The length of chains defines the degree of polymerisation (number of anhydroglucose units) and varies substantially even within one cell wall. Cellulose is a homopolysaccharide and consists of glucose units linked together by glycosidic bonds. Nevertheless, an advanced analysis of the cellulose molecule has resulted in the acceptation of cellobiose as the structural basic unit rather than glucose [20]. It is insoluble in most solvents due to its strong inter and intra polymer hydrogen bonds but remains highly hydrophilic [7,8].

Contrary to cellulose, hemicellulose is a short-chained polymer made of several sugar units (glucose, galactose, mannose, arabinose, xylose, rhamnose) and uronic acids. It is amorphous in structure, soluble in water and easily extractable by dissolution in alkaline medium. Hemicellulose is hydrophilic and surrounds the crystallized cellulose chains within cell walls[7,8]. Lignin is a complex organic polymer of aromatic chains of phenyl-propane responsible for stiffness and impermeability of plant cell walls (hydrophobic). It is mainly found in the middle lamella, the woody-core, and the epidermal and cortical cells of the plant stems [21].

Extractives are made of pectins and non-structural chemicals extractable using polar and non-polar solvents [21]. Pectin is made of units of α-1, 4 galacturonic acid and can be found in primary cell wall and middle lamellae. It is eliminated throughout the retting process of fibres. Pectins are responsible for chemical interactions with hydraulic binders. They attach divalent cations (Ca^{2+}) to form cross linkages between adjacent polymers creating stable gels and hence interfering with setting mechanism. Carbohydrates, lipids, proteins, hydrocarbons, and minerals/inorganic components are present in cell walls albeit at relatively low concentrations compared to holocellulose's, lignin or pectins. The chemical composition varies considerably within different parts and cell walls of a plant. Table 1 shows the chemical compositions of hemp and miscanthus reported from literature.

Insert Table 1.

The chemical composition of bio-aggregates can be assessed using the Fourier Transformed Infra-Red spectroscopy (FTIR). Dasong et al. [27] investigated the chemical composition of a hemp fibre with FTIR and identified the basic stretching bands corresponding to the principal constituents (cellulose, hemicellulose, lignin and pectins). Table 1 summarises the vibration bands and associated chemicals. Chabannes et al. [28] have reported similar hemp shiv FTIR pattern with corresponding mean absorbance peaks.

Insert Table 2.

2.1.2. Microstructural and physical properties

Bio-Based Building Materials inherit all their sought–after properties (hygroscopic-thermal and acoustic insulation) from the porous and lightweight structure of their aggregates. Therefore, this porous structure of the aggregates explains the interest in understanding their internal structure, density, and pore-sizes distribution. The intra-particle voids, which are the vestiges of the dense water and minerals transportation system, constitute the internal porosity of the bio-aggregates. Plant cell walls have specific chemical composition. Their unevenly distributed cellulose fibrils have the potential to affect the overall physico-chemical properties of the aggregates, and hence those of their composites.

From outside towards inside, cell walls are made of middle lamellae, primary cell wall and secondary cell walls. The middle lamellae are mainly made of pectins and provide the bonding between adjacent cells. The primary and secondary cell walls consist of cellulose micro-fibrils (chains of crystallized cellulose) embedded in an amorphous hemicellulose and pectin matrix. The secondary cell wall exhibits high lignin content and specific orientation/tilt angle of cellulose micro-fibrils. These elements display a highly hierarchised structure. The secondary cell wall structure is thought of allowing large shear deformations of cellulose micro-fibrils into the cohesive lignin reinforced hemicellulose matrix [29]. An illustrative 3D structure of a spruce cell wall rebuilt from electron microscopy, x-ray diffractions and atomic force microscopy (AFM) results is provided in [30]. Cell wall microstructure (and pore size distribution) of hemp shiv have been extensively studied using advanced imaging techniques: scanning and transmission electron microscopes (SEM and TEM). It was reported to have identical general structure that is similar to that of miscanthus, with clear foam-like honeycomb structures [31]. Furthermore, it was reported to contain little variations in vessels dimensions (50-80µm) that are surrounded by thick cell walls (~3.0 µm), with a vessel distribution of ~ 20.8 vessels per mm^2.

The undisturbed bulk arrangement of hemp shives/hurds constitutes inter-particle porosity due to the stacking of parallelepiped aggregates. The bulk density, particle density (apparent density) and solid phase density (true density) of the hurds allow the determination of intra and inter-particles porosities [16]. The inter-particle porosity can be further distinguished into several types according to their shape (cylindrical, ink-bottle shaped, funnel shaped) and their accessibility (open, blind, and closed). While the bulk density can be measured straightforwardly, particles and solid densities are relatively delicate to measure. Solid density can be obtained using pycnometric principles (helium, air or C_7H_8) and particle density deduced from the Archimedes law for particle volume determination [32] or through the inter-particle porosity and solid (true) density as shown in equations 1 and 2 [6].

$$\Phi_{inter} = 1 - {}^{\rho_p}/_{\rho_s} \quad \text{(Eq.1)}$$

$$\Phi_{inter} = W_s \times {}^{\rho_s}/_{\rho_W} + (W_s \times \rho_s) \quad \text{(Eq.2)}$$

Where ρ_s is the solid phase (true) density, ρ_p is the particle (apparent) density, ρ_W is the water density and w_s is the water absorption at saturation. Table 2 summaries the densities and porosities of hemp and miscanthus.

Insert Table 3.

The porosities shown in Table 2 (in bold) were calculated using the equations1, 3 and 4.

$$\Phi_T = 1 - {}^{\rho_b}/_{\rho_S} \quad \text{(Eq.3)}$$

$$\Phi_{Intra} = \Phi_T - \Phi_{Inter} \quad \text{(Eq.4)}$$

Where ρ_b is the bulk density, Φ_{Inter} the inter-particle porosity, Φ_{Intra} the intra-particle porosity and Φ_T the total porosity.

2.2. Vegetal fibres/mineral matrix interactions and fibres treatment techniques

2.2.1 Lignocellulosic materials – lime and cement interactions

Scientific literature discussed the chemical interactions between lignocellulosic aggregates and mineral matrices in bio-based composites. These include the disturbance of setting and hardening mechanisms at early ages, modification of basic properties in the mid-age of the hardened composites and durability in the long term [17].

In-depth investigations on the stability and reactivity of the hemp particles in alkaline and calcium-rich medium reported low dissolution rates of sugars (11.4, 17.5 and 22.0 mg/g) and organic acids in water (glucuronic:10.3, 0.6 mg/g and galacturonic acids :5.9 mg/g), lime solution (pH of 12) and $CaCl_2$ solution (pH of 6). The released sugars and acids have an impact on chemical properties of the leachate and interfere with setting and hardening mechanisms of the composites [8]. Sedan et al. [34] reported low dissolution levels of pectin contents. Pectins carboxyl can react with Ca^{2+} ions to form stable gels. The absorption of Ca^{2+} ions constitute a competition for both C-S-H hydration and lime carbonation, in addition to sugars retarding effects [8].

The majority of interaction mechanisms reported concern cement matrix composites, and mechanisms involved in lime and pozzolanic binder matrices can be fundamentally different depending on the alkalinity of matrix pore solution and individual matrix mineralogy, as observed for C_3A and C_3S cement phases [35]. Some of these phases exist in lime-based binders, even though in smaller amounts. Arizzi et al. [36] investigated the chemical, morphological and mineralogical interactions between hemp hurds and aerial and natural hydraulic lime. The authors highlighted high water competition among the constituents causing weak adhesion and delayed hardening process associated to high contents of portlandite, vaterite (μ-$CaCO_3$) and calcium silicates after three months curing period.

Important phenomena occurring in chemical interaction of bio-aggregates with mineral binders at early age and mid-term have been observed in the wood-cement composites science since 80's [37]. Recent literature relevant to this subject include: the influence of sugar cane bagasse fibre on setting of reinforced cement composites [38]; wood-cement interactions and modification of hydration mechanisms [39,40]; the impact of extracted components from aggregates on cement setting and hardening [24], hemp and lime-flash metakaolin binder composites [41]. Although the chemical interactions are the most prevalent, the binder–aggregate interface can be affected by physical phenomena dominated by water flow routes through constituents. This affects associated drying-wetting mechanisms [28] and the shrinkage-swelling of the aggregates influencing the interfacial transition zone.

Studying the curing conditions of hemp-lime composites, Chabannes et al. [28] tested different curing conditions of hemp-lime and evaluated their influence on mechanical properties and composites microstructure, in addition to lime water treatment. Indoor standard curing conditions (ISC: 20°C and 50% relative humidity), moist curing conditions (MC: 20°C and 95% RH) and thermal activation (TA: 50°C and 95% RH) were the applied curing protocols. The scanning electron microscope imaging (SEM) was used to observe the interface zone of the aggregates-binder matrix of hemp-lime composites (HLC) under ISC , MC and TA curing conditions (Fig. 1). Under MC/TA curing conditions, the aggregate-matrix gap thickness increases about 40 times as per ISC curing conditions. This is presumably due to capillary pressure and moisture transport between aggregate and binder [28] similar to those observed in brick-mortar interactions in masonry.

Insert Figure 1. (1.5 column width)

2.2.2. Treatments of lignocellulosic aggregates for bio-based materials

The improvement of aggregate binder compatibility is of great significance for the performance and durability of bio-aggregate concretes. Multiple physical, chemical, and thermal treatment techniques were investigated as attempts to address the incompatibility concerns. Treatment methods can be classified as: (a) physical treatments, intending to prevent water absorption and leakage of chemicals, (b) thermal treatments aiming at the heat degradation of hemicellulose responsible for aggregates swelling and carboxylic acids (glycolic, pyruvic, malic or o-salicylic) release after hydrolysis, and (c) chemical treatments preventing the hydroxyl groups from binding with water or chemical acceleration of hydration kinetics [16,17].

The presence of silica in rice husks has resulted in a pozzolanic effect in composites, and hence, the introduction of silica in aggregates using saturation treatment has been investigated. Coatanlem et al. [42] evaluated the properties of wood chippings - cement concrete with a 24 h aggregate treatment in sodium silicate (100g/l). The use of a binder to aggregate (b/a) weight ratio of 3.0 and water to binder (w/b) ratio of 0.75 resulted in compressive strength of 9.85 N/mm^2 at 510 kg/m^3 unit weight corresponding to a 30.11% improvement compared to water treated aggregates. Ettringite needles were observed at the surface of silica-treated aggregates as a consequence of improved bonding between aggregates and cement matrix.

Olorunnisola [43] investigated coconut husk-cement composites (particleboards) and the effects of calcium chloride on mechanical properties. Calcium chloride was used as an accelerator to counterbalance the inhibitory effects of coconut husks on cement. The use of 3.0% $CaCl_2$

resulted in compressive strengths (for 0.85 mm sieved fibres) of 2.6 N/mm^2 for untreated aggregates (896.8 kg/m^3) and 4.1 N/mm^2 for calcium chloride treated aggregates (942.7 kg/m^3). Compared to untreated specimens, the results show 57.69%, 47.85% and 57.14% increases for compressive strengths, modulus of elasticity and modulus of rupture, respectively.

Although sucrose is considered a cement retarding agent as it accelerates ettringite development while retarding the hydration of tri-calcium silicate (C_3S), cement - sucrose coating of flax shives improves flax shives concrete properties [44]. The addition of large amounts of sucrose resulted in opposite effects to those of small sucrose quantities (1-3%), i.e. the increase of compressive strength (0.4 to 3.5 N/mm^2) and the reduction of setting time. The retarding effect limited the amount of sucrose to be included at 40 wt % of cement. This treatment, when applied to flax shives, reduces the absorption of water from 200% to 54% and results in a 50% reduction of drying shrinkage [44].

In an attempt to reduce the dimensional variations of wood sand concretes, Bederina et al. [45] explored various wood shaving treatments and their impact on mechanical and thermal properties. In their study, cement and/or lime coating and oil impregnation were investigated. All the evaluated treatments methods resulted in reductions of dimensional variations, and shrinkage reductions of 43.6% and 35.9% reported for oil and lime treatments leading, respectively. Cement and cement-lime treatments reduced shrinkage by 25.6% and 28.8% respectively. The compressive strength improved from 23% for lime treatment to 58% for cement treatment. However, these evaluated treatments did not improve the thermal insulation of the wood-sand concretes. On the contrary, the thermal conductivity increased by 14% for cement treated wood shavings.

Le Troëdec et al. [46] investigated numerous physico-chemical treatments of hemp fibres and their effects on the interaction of fibres with lime matrix. The use of combined Scanning electron microscope (SEM), x-rays diffraction (XRD), differential scanning calorimetry (DSC) and FTIR analytical techniques allowed to evaluate different treatments of fibres including: alkali treatment for 48 h in an NaOH solution of 0.06 M; immersion in a solution of 5.0 g/l - 0.06 M ethylene diamine tetra-acetic acid (EDTA :pH of 11) for 3 h; soaking in a solution of 2000 g/mol of poly-ethyleneimine (PEI) for 48h and saturation with lime (pH of 12.7). The treatment of fibres with a NaOH solution of 0.06 M improved their crystallinity through the hydrolysis of amorphous compounds resulting in high rigidity of the composites. EDTA and PEI reacted with calcium ions adsorbed on pectins and carbonyl groups of cellulose, increasing the crystallinity of fibres and the stiffness of composite [46].

Chabannes et al. [28] investigated the effects of lime-water treatment on hemp shives. The lime-treatment reduced by half the compressive strength of samples :0.44- 0.22N/mm^2. From FTIR analysis results, the authors reported leaching of polysaccharides as a result of strong disintegration of the primary cell walls. The most remarkable disintegrations included the disappearance of 1730 cm^{-1} band corresponding to unconjugated C=O bond of the hemicellulose's xylan; a decrease of 1030 cm^{-1} peak associated with C-C,C-OH and C-H cellulose and hemicellulose rings and disappearance of 895 cm^{-1} and 1370 cm^{-1} bands attributable to polysaccharides glycosidic bonds and in plane C-H bonding of polysaccharides, respectively [28].

Accelerated carbonation or fibres treatment in slurred silica fume / blast furnace slag are some of the methods to improve the durability of lignocellulosic fibres (sisal and coconut) in the alkaline medium that is generated by the hydration of cement [47]. The authors concluded that immersing fibres in silica fume slurry reduces long-term embrittlement of composites. The investigation of silica treatment of hemp shives using tetraethyl-orthosilicate (TEOS), nitric acid, hexadecryltrimethoxysilane (HDTMS) and absolute ethanol in the sol-gel process resulted in 250% reduction of water absorption [48]. Moisture absorption was reduced by 30% with a maximum moisture content of 12.81% and 19.68% for coated and uncoated shives at 90% relative humidity [48]. Ramlee et al. investigated the impact of silane (triethoxy-ethyl) and hydrogen peroxide (H_2O_2) treatments on oil palm empty fruit bunch and sugar bagasse, for potential use in thermal insulation materials [49]. A 2% silane treatment removed hemicellulose and lignin, as observed using coupled SEM-FTIR analysis, and resulted in an increase of tensile strength. Furthermore, the authors reported that 4% H_2O_2 silane treatment enhanced the bonding of fibres to the resin matrix. In a comparable study on the effects of alkali (NaOH) and/or silane (triethoxy-ethyl) treatments on kenaf and pineapple fibres, Asim et al. [50] reported an increase of strength and removal of hemicellulose and lignin.

Calorimetric analysis suggested that miscanthus had little effect on cement hydration. The only concern was the high-water absorption of miscanthus [47]. Different methods to improve the compatibility of cement and miscanthus fibres (in terms of water competition and adhesion) were proposed: (a) modification of the cement matrix using pozzolanic materials that reduce its alkalinity; (b) modification of fibres using pre-saturation, cement - slag impregnation (0.5 w/b and 2.0 b/a), immersion in sodium silicate (water glass) at 50% dilution (100 ml Na_2SiO_3 / 200 g H_2O and 50 g fibres), acting both as a water reduction agent and providing rough surface, lignin coating, linseed oil impregnation (2.0 linseed oil/ fibre ratio) and thermal treatment (hornification). The water absorption at saturation was reduced to 140% for water glass treatment, 180 – 200 % for linseed oil and 215% for cement treatment compared to 300% for untreated fibres. The treatment of fibres using lignin provided limited improvements.

The production of cementitious composites using residues of miscanthus enzymatic saccharification (cellulose, β glucosidase and xylanase) preceded by chemical treatments (2% H_2SO_4, 121°C for 1h and 33% NH_3, room temperature for three days) was investigated in [51]. Both treatments resulted in a reduction of lignin and cellulose-hemicellulose content of fibres. Nevertheless, the chemical treatment increased water absorptions (525-550%) with reference to untreated aggregates (300%), six times higher setting times were reported, and 62% reduction of compressive strength (without significantly impacting the flexural strength).

The alkaline treatment of bamboo fibres using a 4.0 wt% NaOH solution at 20:1 volumetric ratio for 1 h was proposed in the literature. Zhang et al. [52] used thermogravimetric analysis (TGA) and differential scanning calorimetry (DSC) to highlight modifications in the chemical structure of fibres. Treated fibres exhibited a higher thermal stability than untreated fibres, confirming a decrease of hemicellulose, lignin, and pectin content. The FTIR results corroborated the foregoing statements with the removal of hemicellulose and lignin that increased the relative amount of cellulose. Furthermore, an alkaline treatment was applied to Ensete fibres to reinforce a polymer matrix as described in [53]. The authors investigated the treatment of fibres using 2.5%, 5.0% and 7.5% NaOH solution for the reinforcement of unsaturated polyester and reported mechanical improvements in the order of 14.5% and 43.5% for flexural and Young modulus, respectively. Additionally, the observed shifting of glass transition temperature and the SEM microstructural observations confirmed enhancements of fibre-matrix interface. The increased performance of alkali-treated fibres is linked to the removal of hemicellulose/lignin and the increased rough surface area available for the bonding of fibre - matrix. These elements are valuable for both mineral and organic binders.

The use of vegetal fibres in conjunction with mineral binders such as Portland cement remains challenging. A recent review reported substantial advancements considering a wide variety of proposed treatments to address the problems related to fibre-matrix compatibility [54]. However, most of these treatments exhibit little practical potential due to the economic, safety and environmental aspects of the involved chemicals. This is one of the many drawbacks that favoured the use of lime-based mineral binders in preference to cement in bio-based building materials.

2.2.3 Interactions of lignocellulosic materials and alkali - activated binder matrices

- Geopolymer-lignocellulosic composite materials constitute a relatively recent research subject and most of the scarce literature available covers the reinforcement of geopolymer matrix with vegetal fibres. A limited number of studies investigated wood-geopolymer concretes. Nevertheless, fundamental chemical processes involved should be theoretically the same for both fibres and particles interactions with geopolymer matrix. Korniejenko et al. [55] studied the mechanical properties of fly ash geopolymer composites (8.0 M NaOH + Na_2SiO_3) reinforced with natural fibres (cotton, raffia, sisal and coir/coconut fibres). The cohesion of natural fibres examined through SEM revealed voids around the coir, raffia and cotton fibres as shown in Fig. 2. A Comparable phenomenon was observed for flax fibres in cement matrix (Fig. 3) [56] with different chemistry though. Nevertheless, compressive and flexural strengths of reinforced composites remained relatively higher than those of non-reinforced materials. The fibres occupied 1% volume of the matrix and the incorporation of higher proportions of fibres and the increase of fibres dimensions resulted in reductions of strength.

Insert Figure 2. (1.5 column width)

Insert Figure 3. Single column width

Chen et al. [57] observed well-coated and void surrounded fibres in their study of sweet sorghum bagasse fibre for the reinforcement of fly ash-based geopolymer. However, the authors did not provide an explanation for the observed phenomenon. Results on fresh properties, mechanical strength and microstructure of fly ash geopolymer paste reinforced with untreated sawdust (~2.0 cm long and 790 kg/m^3 bulk density) at ratios of 5-20 wt% are reported in [58]**.** Conversely, sawdust inclusion up to 20% in the concrete improved both strength and microstructure. The main reported results are:

- The incorporation of sawdust (SD) reduced workability at ratios exceeding 5% (150- and 113-mm slumps at 0 and 20%SD respectively) and significantly increased the setting time (425 and 600 min at 0 and 20% SD respectively);
- The sawdust reduced cracking and drying shrinkage (~35.21% at 14 days for 20%SD);
- Compressive and flexural strengths improved by ~16.6 and ~ 31.58 % respectively for 20%SD (1600 kg/m^3) at 28 days of curing (40°C/24h - 20±2°C and 90±5% rh);
- The microstructure of SD geopolymer composites, investigated using SEM micrographs, exhibited better features, such as the absence of micro-cracks for SD composites. The strength improvement was associated to the enhanced pore structure of the composites with a decrease of both pore sizes < 50 μm and critical pore diameters (~20 and 50 μm for 20 and 0%SD respectively).

Sarmin and Welling [59] studied lightweight composites of wood particles (3 - 5 mm) and class F fly ash – metakaolin alkali-activated binders. The compressive strength was increased by 62% for a 10wt% wood incorporation compared to 0wt% wood composites. Furthermore, the field emission scanning electron microscope images revealed a dense wood/gel geopolymer matrix interface with wood particles fully embedded in the aluminosilicate matrix. Through the reported literature, weak interface zone was identified for fibres - geopolymer matrix system [55]. While a volumetric concentration of fibres exceeding 1.0% reduced strengths [55], the use of 20wt% sawdust increased strength in [58]. A direct comparison across various studies is not straightforward: matrix microstructure, curing conditions and different surface areas due to the fibres and sawdust incorporations explain the encountered differences in compressive strength trends.

3. Bio-based building materials mix design and manufacturing techniques

3.1 Mix design and manufacturing techniques of bio-based building materials

Mixes of construction materials incorporating biomass / vegetal derived aggregates are difficult to design due to high water absorption and compressibility of the aggregates and the influence of the binder on the compactness of the aggregates. Various approaches can be used for the purpose mix of design. In their study of rice husk-cement composites, Doko et al. [60] proposed the use of absolute volume approach. The absolute volume of fresh composite mix ($V_{abs.Comp}$) is calculated from the sum of absolute volume of cement ($V_{abs\,cement}$), rice husks aggregates ($V_{abs\,.aggr.}$) and water (V_{water}) according to equations 5 et 6.

$$V_{abs.Comp} = V_{abs\,cement} + V_{abs\,.aggr.} + V_{water} \qquad \text{Eq. 5}$$

$$V_{abs\,cement} = {C}/{\rho_C}\,;\; V_{abs\,.aggr.} = {a}/{\rho_a}\,;\; V_{water} = {k_w C}/{\rho_w} \qquad \text{Eq. 6}$$

Where C is the mass of cement, a the mass of aggregate, ρ_C the specific density of cement, ρ_a the specific density of the aggregates, ρ_w the specific density of water and kw the water to cement mass ratio (w/c). The mass of the aggregate of the mix was calculated considering a unit absolute volume of fresh composite mix $V_{abs.Comp} = 1$ as shown in equation 7.

$$A = \rho_a \left(1 - {C}/{\rho_C} - {k_w C}/{\rho_w}\right) \qquad \text{Eq. 7}$$

Akkaoui [61] proposed a mix design method for wood-cement composites, assuming that the binder has no influence on the compactness of wood aggregates. This applies for low volumetric proportions of binders (lower than the volume of intergranular pores of the aggregates). Considering the compactness of wood at 0.38, the mass of the aggregates was estimated: $A = \rho_{abs} V_A C_A$ (where V_A the total apparent volume of aggregates, C_A the compactness and ρ_{abs} the absolute density of the wood aggregates). The mass of binder and water were calculated from the ratios of cement to aggregate (1.25 – 2.75) and water to cement (0.5). The volume of cement paste and the volume of inter-granular pores were estimated respectively from equations 8 et 9.

$$V_{cp} = {}^{C}/_{\rho_C} + {}^{W}/_{\rho_W} \qquad \text{Eq. 8}$$

$$V_p = V_A(1 - C_A) - V_{cp} \qquad \text{Eq. 9}$$

Where $V_{cp}$is the volume of cement paste, V_p volume of the pores, C the mass of cement, ρ_C the density of cement, W the mass of water and ρ_w the density of water.

Chabi et al. [18] proposed a method for the design of rice husk-cement concrete considering aggregates as ‘suspended’ into a continuous matrix of mineral binder. The volume of the aggregates was estimated from the application of the Compressible Packing Model (CPM) and the volume of cement and water calculated from the Feret’s equations (equations 10 et 11) for concrete mix design (a compactness value of 0.4 was retained considering a compactness index of K of 3).

$$\sigma_{c28} = KF\left({}^{c}/_{c + w + a}\right)^2 \qquad \text{Eq. 10}$$

$$V_a + f + c + w + a = 1.0 \qquad \text{Eq. 11}$$

Where KF is the constant for the quality of binder, and c the volume of cement, w the volume of water, a the volume of residual air and Va the volume of the aggregates.

Nguyen [10] proposed another method of mix design for hemp concrete using a targeted initial density (hence final dry density), a fixed binder to aggregate mass ratio (b/a) and water to binder mass ratio (w/b). Considering a fixed initial fresh density of hemp concrete ρ_{in}, the mass of aggregate (a) was calculated from equation 12. The mass of binder was obtained from b/a ratios (1.11, 2.15 and 3.48) and that of water from w/b ratios (0.55, 0.86 and 0.93).

$$\begin{cases} \rho_{in} = a + b + w \\ a = \rho_{in} / \left(1 + \left(b/a\right) + \left(w/b\right) \times \left(b/a\right)\right) \end{cases} \qquad \text{Eq. 12}$$

The mix proportioning of hemp-lime concretes depends on the manufacturing processes and the intended materials use, hence, fixing an initial target density allows to determine the constituents mass and /or volumes from their unit weights [10]. From the same principle, other approaches based on compactness were successfully developed for wood-cement composites [59] and rice husk-cement composites [60].

Specimen manufacturing techniques applied in different studies intend to simulate materials manufacturing at the factory/building construction level: manual casting - tamping for on-site wall construction; compaction and vibro-compaction for wall panels and hemp bricks pre-casting; and projection for onsite walls and roof panels. For the manual tamping manufacturing technique, the b/a ratio ranges from 1.5 to 2.5 [16]. Compaction and/or vibro-compaction is applied to reduce the total inter-particle voids, increase density and ensure minimum required strength. These techniques allow to increase the final density and to reduce the b/a and w/b ratios for mix designs. Additionally, higher aggregate content can be used to achieve low thermal properties [10,12].

summarises mix design methods depending on manufacturing process and curing regimes in comparison to the French reference recommendations for hemp concrete ‘Construire en Chanvre’ [62].

A detailed schematic illustration of hemp- lime applications in a building is shown in [11]. In the UK, the main use of hemp-lime is for non-structural applications in walls [61]. The actual trend is the manufacturing of load bearing blocks using high compaction pressures. The compaction process has evolved from pressures about 2.80 N/mm^2 for hemp-lime [10], 5.0 N/mm^2 for hemp and sunflower aggregates in pumice – lime binder matrix [63] and 10 N/mm^2 for hemp – lime composites [64]. A special device was developed for the compaction of fresh mixes in [16] to adapt a Φ11 x 22 cm^3 mould that is filled in three steps using layers of measured materials according to the desired density. This equipment can be adapted to cubic moulds. For higher compaction pressures, the equipment described can be connected to a hydraulic transmission machine. This system was applied to hemp-lime samples using a compacting device in PVC designed for the application of 0.1-2.0 N/mm^2 stresses in Φ100 x 200 mm^3 moulds [10]. Tronet et al. used a modified device to apply a pressure of 10 N/mm^2 in the midst of hemp concrete casting [64].

Vibro-compaction is a manufacturing process combining compaction at specific stress and perpendicular direction vibration of samples at specific frequencies. Soil vibro-compaction device (VCEC from MLPC®) was adapted to accommodate Φ100 x 200 mm^3 cylindrical hemp and rice husk - lime concrete samples [16]. This equipment was used to cast samples of of Φ160 x 320 mm^3 for compressive strength testing with applied compaction pressure of 0.6 N/mm^2 and a 30 seconds vibration period [63]. In addition to differences in individual materials mixing steps, demoulding and curing conditions vary from one study to another as reported in

. Common binder formulations used in conjunction with bio-based aggregates are shown in Table 5.

3.2 The influence of mix designs on physical properties

The properties of bio-based composite materials depend on several parameters. In addition to the manufacturing techniques, the weight ratios of constituents (water to binder: w/b and binder to aggregate : b/a) constitute basic mix design parameters that influence final mechanical and thermal properties of composites. Data from literature shows that various mix designs incorporating different types of binders exhibit linear correlations of density and both binder to aggregate (b/a) and (w/b) ratios (Fig. 4) [6,65,66]. The application of high compaction stress values results in outliers as shown in Fig. 4.a). The mixing water of the composite (water to binder ratio) depends on the nature of aggregates which is highly water absorbent with rates of absorption ~ 220-280 % in 5 minutes [6,7,10,65]. In fact, high content of aggregates (low b/a) requires high amounts of water (w/b) in the range of 0.9-2.0 and leads to low final densities (250-550 kg/m^3) as illustrated in Fig. 4.b).

Insert Figure 4 (1.5 column / width: 120 mm)

Insert Table 4.

Insert Table 5.

4. Mechanical properties of bio-based materials

4.1. Compressive strength – density relationships and evolution as a function of formulations and manufacturing techniques

The most studied mechanical property of bio-based materials is their compressive strength, its correlation with the weight ratios of constituents, the unit weight of composites and porosity. The morphology of hemp hurds reveals high internal porosity [65] with reported value of 57.0% using 3D tomography. Similar porosity values are reported: ~ 59.90% for hemp [10] and 52.24% for miscanthus particles (calculated from particle and skeleton densities)[32]. High porosity aggregates lead to high porosity composites resulting from both the internal structure and bulk arrangement of particles. The binder matrix itself presents high porosity (~50% for lime-based and ~ 39% for Portland cement). The latter influences the density of the composites and its compressive strength. Hence, considering aggregates and binders, the parameters affecting the mechanical properties of hemp concretes include mix design proportions, curing conditions and age, binder content and the particle size distribution of aggregates. The influence of these parameters has been covered [65] and reported results can be summed in three points:

- Bio-based building materials (BBBMs) present low compressive strength and high deformation values under compressive stress, limiting hemp concrete to non-structural applications.
- The higher the binder content, the closer the mechanical behaviour of hemp concretes to that of pure binder paste.
- Neither high humidity curing (75% and 98%rh) nor low humidity curing (30%rh) are suitable for hemp concretes as they slow down the setting of hydraulic lime binder.

The evolution mechanical compressive strength as a function unit weight and mix composition was analysed from literature data (Fig. 5 a). In fact, as shown in Fig. 5 b), the effect of unit weight on compressive strength of samples can be attributed to the binder content of composites [6]. On the other hand, from the experimental results in [10], it was observed that different values of density can be obtained from similar b/a ratio mixes as illustrated in Fig. 6. The linear correlations of binder content, strength and density can be obtained for tampered concrete (Fig. 6 a) in contrast to the compacted concrete (Fig. 6 b).

Insert Figure 5 (Double column / width: 185 mm)

Insert Figure 6. (Single column/ Width 90 mm)

Macroscopic porosity regulates the density of samples and the application of high compaction pressures (0.30 – 2.89 N/mm^2) explains that difference from un-compacted samples (Fig. 6 a). However, in both cases the density remains the principal factor influencing strength. Considering low weight materials (no compaction), the strength of binder matrix itself controls the strength of composites since the aggregates will not transfer loads. The same b/a values, considering different types of binders, result in composites with different strength values (0.025 – 0.175 N/mm^2) for composites of ~ 250 kg/m^3 [67]. Hemp-lime mixes of b/a ratio of 2.15, initial unit weight of 860 kg/m^3 and water to binder (w/b) ratio of 0.86 containing different binders (Natural hydraulic lime, Ordinary Portland Cement and Tradical PF70) were investigated in [10]. Strength values reported at 7.5% strain and after 28 days of curing were 2.5, 2.3, 1.5 and 1.45 N/mm^2 respectively.

It was shown that volumetric proportion of paste controls the development of strength in hemp concretes. An increase in paste volumetric proportion by 30% increases the compressive strength by 360% [6]. However, Nguyen [10] reported a reduction of strength as the b/a ratio increased while keeping the same unit weight and w/b ratio. In fact, low b/a ratio imposes high compaction of aggregates to achieve unit weight similar to that of mixes with high b/a, resulting in higher strength values. Table 6 summarises some basic mechanical properties of low to medium density hemp-lime composites.

Insert Table 6.

4.2 Stress – strain behaviour of BBBMs

The analysis of stress-strain curves of hemp concretes provides valuable information about the mechanical behaviour of hemp concretes. In fact, depending on the mix designs, hemp concretes show a strain hardening - plastic behaviour and a comparative analysis of mechanical behaviour of different formulations is only achievable through benchmarked strains [10]. From the analysis of the stress-strain behaviour using the observation of optic deformation fields, a classification of mechanical behaviour was defined and reference strains set at 1.5% (the upper end of the linear elastic behaviour) and 7.5% (the limit of strain hardening) as illustrated in Fig. 7 [10]. The four major steps of hemp-lime typical stress-strain kinetics with controlling mechanisms were identified as:

i) the initial elastic zone corresponding to matrix response to loads;
ii) the elasto-plastic zone corresponding to a progressive cracking of the matrix at the interfacial transition zone (ITZ);
iii) the strain-hardening plastic zone corresponding to aggregates compaction - cohesion and;
iv) the eventual rupture peak and stress recession appearing for high binder containing formulations.

Insert Figure 7. (Single column / width: 90 mm)

These observations were confirmed by Cérézo[6], highlighting the bi-phases mechanical behaviour of hemp concretes. The author described an initial linear elastic behaviour followed by a second elasto-plastic phase. The latter having an inflexion of the stress-strain curve under the crack development in the matrix (non-linearity) and residual strains under cyclic loading. The importance of the compaction has been highlighted since the compressive strength increases with compaction level and this is reflected by the initial unit weight for identical b/a and w/b ratios [10]. The binder content is an additional influencing parameter over the mechanical behaviour of hemp-concretes.

Mazhoud [33] and Kioy [71] reported similar behaviour with a distinction between composites of high and low content binder, the latter presenting no stress peak at large strains. The peak of stress – strain curves identifies the transition from binder matrix load transfer path to fibre - cohesion load transfer path. The foregoing mechanical descriptions highlight the particular effect of binder content on the stress-strain behaviour and failure mechanism of hemp lime composites (HLC) [4]. Niyigena reported a highly distinguishable fragile behaviour of composites with high binder content versus a ductile behaviour of composites with low binder content [85]. The author reported the values of strain in the range of 4.0- 15 % for 10-40 v/v% binder content (compared to strain of 1.2% for pure binder). The literature [6,10,65], corroborates the aforementioned trend and behaviour similar to the mechanical profile of pure binder for composites with high content of binder versus a behaviour similar to that of pure aggregates for composites with low content of binder.

Insert Figure 8. (Single column)

Additionally, the stress-train behaviour of lime-hemp concrete (LHC) depends on the applied compaction stress at the mixing process. The application of compaction stresses in the range of 0.05 – 2.5 N/mm^2 distinguishes the strain - softening from strain - hardening failure mechanisms [10]. Tronet et al. [64,73] showed that, as for most of the building materials, the most important factor affecting strength remains its compactness in the hardened state, which depends on water content and compaction at fresh state as shown in Fig.8. The compactness threshold of 0.25 was found the limit at which the binder matrix is no longer the sole parameter controlling the compressive strength. Tronet et al. [73] developed a mechanical model that considers the mix design and casting process. Equation 13 was proposed for a 28-days compressive strength based on power law principle (application boundaries are $S > \rho_B$ and $B/_S < 5.42$).

$$\sigma_y = \sigma_B (B \times K)^a + \sigma_S \left(S\left[{}^1/_{\rho_S} + \left({}^B/_S\right)K\right]\right)^b \;;\; K = \left({}^1/_{\rho_B} + {}^{t-1}/_{\rho_w}\right) \qquad \text{(Eq.13)}$$

With σ_B the specific strength of binder, K is adapted from the volumetric solid fraction of the binder, ‘a’ constant (computed from compression tests on binder at various w/b ratios and equals to 2 for cement and 3 for lime), ρ_B the specific density of the binder, ρ_s the specific density of the shiv, ρ_w the density of water, B and S the binder and shiv masses in a cubic metre of material, b the fitting parameter, t the hydration degree (1.0 for aerated lime and 1.25 for Portland cement).

Williams [66] proposed an empirical relationship between strength and constituents weight ratios (Eq.14) based on internal structure, and considering the binder as the sole contributor to strength. The author used a weighted mean of optimized and minimized arrangements of the binder in a cross section of composite. This internal structure is described by a shape factor (Eq.15), a function of mean particle aspect ratio, mass of the binder, interquartile range of particles sizes, proportion of particles in the primary axis and compaction ratio.

$$\sigma_{CC} = S_C\sigma_{C\perp} + (1 - S_C)\sigma_{C\parallel} \quad \text{(Eq.14)}$$

$$S = F\left(\Phi_p, B, V_{pi}/V_p\,, IQR_p, C\right) \quad \text{(Eq.15)}$$

With $\sigma_{C\perp}$ and $\sigma_{C\parallel}$ idealized series and parallel cased basic models, S_C the shape factor in the loading direction. The shape factors in parallel and perpendicular loading directions were applied to weighted arithmetic means of series and parallel basic models, as illustrated in equation 14, and resulted in a predictive empirical model.

4.3 Flexural strength of bio-based building materials

Flexural strength represents an important mechanical property of building materials as it defines the ability of the material to resist bending stresses for load-bearing materials and handling stresses for non-load bearing materials. Pavia and Walker [86] studied the flexural behaviour of different hemp-lime composites at 7, 28 and 90 days of curing. The lime-hemp composites were made of hydrated lime and a pre-formulated commercial binder (hydraulic lime and pozzolanic additions) mixed with hemp shivs at b/a volumetric proportions of 0.33, 1 and 9 (respectively for wall, floor and plastering applications). It was observed that flexural strength increased with the increase of volumetric proportion of binders generally. An increase of commercial binder proportion from 25 to 50% increased flexural strength by 12 times at 7 days (0.25 to 3.0 N/mm^2) with no further impact on flexural strength for an increase up to 90% of binder. Composites with high proportions of commercial binder (TH10 and TH50) have higher strength and brittle behaviour while lime-based composites (CL90H10, CL90H50 and CL90H75) generally have lower strength (increasing with binder proportion) and a ductile mode of failure. Williams [66] reported flexural strength ranging from 0.14 N/mm^2 to 0.33 N/mm^2 for hemp-lime composites of density of 379-431 kg/m^3.

4.4. Mechanical anisotropy and shear strength of bio – based materials

Hemp-lime is an anisotropic material with preferential orientation of the aggregates in the direction perpendicular to the direction of compaction force. It can be appreciated from literature [72] that hemp-lime composites exhibit higher stiffness and brittleness in perpendicular direction compared to parallel direction of compaction. The authors presented the results obtained for an HLC of b/a 1.18 and 2.6 in both loading directions and confirmed a brittle strain-softening behaviour in perpendicular direction and a more ductile strain-hardening behaviour in parallel loading direction. Williams et al. [87] corroborated the former statements. Parallel loading yields higher strength values both in compression and flexure at high strains with higher values corresponding to higher b/a ratios.

The analysis of compressive strength values of BBBMs across different studies might be impractical owing to differences in materials and manufacturing processes. Nevertheless, according to results and perceiving observations from literature, it can be assumed that anisotropic mechanical behaviour applies to other bio-aggregates composites manufactured using external compaction/vibration or projection techniques. Although used as a non-load bearing infilling material, LHCs contribute to the mechanical performance at the structural scale for the in-plane racking resistance [88–91]. Investigations on the shear strength of LHCs were conducted at the material scale, using an adapted triaxial testing equipment [92] and a special shear box test [74,93]. Chabannes et al. investigated a 90 days shear strength of the LHC (b/a ratio of 2.3, w/b ratio of 0.8 and fresh unit weight of 975 kg/m^3) under increasing confining pressures (50 – 150 kPa) [92]. The authors reported a peak friction angle of 46° and a cohesion of 355 kPa. Increasing the confining pressure led to the increase of the peak deviatoric stress and a stronger strain-hardening ductile behaviour of the composites. The observed mode of failure was a combination of bulging and shear banding.

5. Thermal properties of bio–based materials

The thermal performance of a building envelope is associated with the thermal conductivity of materials and thermal transmittance (U-value) of wall assemblies, which are good indicators of thermal performance in steady conditions. The majority of literature covers the experimental and modelling of thermal conductivity of BBBMs as discussed in section 5.1. Still, considering real environmental conditions, constantly changing temperatures impose predominantly a transient state in walls. Studying the hygrothermal performance of hemp-wall, Shea et al. [94] reported ~240 hours period, for a 300 mm hemp-wall, to reach steady state conditions from a -20ºC temperature change and a 17% variation of energy consumption compared to steady state. This confirms that U-values method for the evaluation of energy performance of BBBMs of buildings remains arguable. It was shown that dynamic thermal performance simulations and measurements improve the accuracy thermal performance assessments in [11]. The thermal diffusivity and effusivity discussed in section 5.2, are some of the hygro-thermal properties involved in dynamic thermal performance assessments.

5.1 Thermal performance of BBMs in steady state conditions: thermal conductivity

It can be assumed from literature that important specific parameters affecting the thermal conductivity of hemp concrete are the density, moisture content and the method of manufacturing of materials. In addition to influencing strength, density controls the thermal and acoustic properties of bio-based materials as it is related to pore structure of these materials [95]. Porous composite materials with specific pore size distribution must be considered separately. In fact, the predominance of certain pore sizes can affect heat transfer mechanisms, moisture transfer and condensation at the microstructural level and, hence influence the thermal properties [96]. Fig. 9 a) shows the evolution of thermal conductivity as a function of unit weight for projected LHC [69] and compacted LHC [10] with differences attributable to internal structure of the composites as a function of the manufacturing techniques.

Hemp concrete is an effective insulating material with thermal conductivity values of 0.05 – 0.20 W/m.K depending on specific internal structure, density and moisture content of the composite [97]. Thermal conductivity highly depends on the pore size and internal structure of the composite materials. Air enclosed within pores with very low thermal conductivity (~ 0.025 W/mK at 20°C) is responsible for the insulating behaviour to the composite. The results reported from different studies [6,10,69,87] highlight a linear evolution of thermal conductivity as a function of unit weight. Composites with low density (< 300 kg/m^3) exhibit low values of thermal conductivity (0.06 - 0.08 W/mK) while those with medium density (300-550 kg/m^3) show thermal conductivity values in the range of 0.08 - 0.12 W/m.K. Comparable results were reported with thermal conductivity values of 0.12 – 0.160 W/mK for unit weights of 400 – 500 kg/m^3 [97].

The impact of compaction direction was investigated in different studies [7,10,41] preceding the development of empirical [87] and analytical models [98]. Compaction induces high anisotropic internal structure of composites to resemble that of natural wood. Similar results have shown high values for thermal conductivity measured in the direction perpendicular to the compaction direction. Fig. 9 b) shows the values of thermal conductivity of LHC in both parallel and perpendicular directions to compaction direction. Reported results show that thermal conductivity in a direction perpendicular to the compaction is higher than that in parallel direction. The ratio of perpendicular to parallel values of thermal conductivity (range of 1.01–1.80) is attributable to the nearly horizontal direction of aggregates inside the concrete and the anisotropy of the aggregates themselves [10,12]. Investigations on the effect of compaction levels have highlighted that high compaction leads to higher thermal conductivity values in perpendicular direction compared to un-compacted samples in dry unit weight range of 450 – 650 kg/m^3 [16].

However, lower thermal conductivity values in the parallel direction were recorded, compared to values obtained on manually tampered samples in the same direction.

Insert Figure 9. (Double column)

In addition to the density and compaction direction, humidity has an influence on the thermal conductivity of hemp concrete. Cérézo [6] measured the thermal conductivity of hemp concretes at 50 and 75% RH and compared them to measures at 0% RH with a noticeable impact of elevated humidity values on thermal conductivity. From the reported results, clear distinguishable three zones were identified. For first zone of density values in the range 200-300 kg/m^3, the thermal conductivity increases by 41.6 % (0.06 to 0.085 W/m.K) for humidity increase from 0% to 50% rh and an increase of up to 83.33 % for 75% rh with thermal conductivity reaching 0.11 W/m.K. This range of density values remains the most sensitive to humidity change. The second zone corresponds to density range of 300 – 450 kg/m^3. An increase of the thermal conductivity of 10% and ~ 40.0% were recorded for the humidity from 0 % RH to 50% RH and 75% RH, respectively. The third zone considers values of density higher than 650 kg/m^3 with an increase of thermal conductivity of 15% from 0 to 50% RH. It is obvious that for all values of humidity, the thermal conductivity is higher than for 0% RH. In fact, with regard to the Kelvin - Laplace law of capillary condensation, the higher the rh, the lower the minimum radius required for condensation, increasing the amount of pore water [99]. The capillary water is responsible for the rise of thermal conductivity at high rh conditions given the high thermal conductivity of water (0.59W/mK compared to 0.025 W/mK for air at 20°C). Comparable results (Fig. 9 c) were obtained by Collet and Pretot [97].

Gourlay et al. [100] reported that water content can reach 10wt% for hemp concrete at 50% RH and ~ 25% at high levels of humidity (95% RH). An increase in water content linearly increases the thermal conductivity of hemp concretes. This supports the hypothesis of condensation water in pores which increases the thermal conductivity of hemp concretes. Comparable relationships of water content - thermal conductivity have been reported in literature [97,99,101].

Hamilton and Crosser [102] conducted the earliest studies on the thermal conductivity of heterogeneous two-components systems. Thermal conductivity models for hemp-lime were developed using the self-consistent scheme model [6] inspired from the studies on autoclaved aerated concrete [103]. The other homogenization techniques (Mori-Tanaka and Halpin Tsai) along with the self-consistent model were tested on hemp concrete [104], and later a multi-scale homogenization approach was applied on LHCs [105]. Tran-Le et al. [98] developed an anisotropic analytical model for the determination of the effective thermal conductivity tensor of hemp-lime, considering various preferred spatial distributions of hemp particles. Dartois et al. [106] applied an iterative micromechanical model for both thermal and mechanical properties of hemp-lime taking into account the shape and orientations of 'parallelepiped' particles. Mom [107] developed a non-linear 3D resolution-enriched homogenization model for hemp concrete. Thermal [14,96] and hygrothermal [15] performance studies of the hemp – lime at the building scale allow an upscaling of the foregoing numerical and experimental studies.

5.2 Thermal performance of BBBMs in transient conditions: heat capacity, thermal diffusivity and effusivity.

The heat capacity of a material measures its ability to store energy. It is defined by the amount of heat required to increase by unit degree of temperature a unit mass of the material. A high specific capacity allows to delay and dampen heat waves through a material. The phenomenon is referred to as thermal mass or thermal buffering and can significantly influence energy performance estimations of buildings [108]. The specific heat capacity intervenes in the determination of thermal diffusivity, which assesses the rate of heat transmission through a material in a temperature-varying environment, considering its ability to store and exchange heat energy. The thermal diffusivity is the ratio of thermal conductivity to the product of density and specific heat capacity [109]. Even though these properties allow accurate determination of thermal performance of whole buildings, in the context of BBBMs, the data remains largely limited compared to steady state thermal performance.

Hemp concrete has a relatively high heat capacity considering its low density. Collet-Foucault reported specific heat capacity of 1.0 kJ/kg.K for a density of 392.9 kg/m^3 [5]. Walker and Pavia reported a comparable value for hemp-lime (1.068 kJ/kg.K) for slightly higher density (602 kg/m^3), and Mazhoud et al. reported similar values in the range 0.99-1.01 kJ/kg.K for even denser hemp-lime plasters (723-881 kg/m^3). Slightly higher value (1.56 kJ/kg.K) were reported for a hemp-lime having a dry density of 480 kg/m^3 in [11]. Reilly et al. reported a specific heat capacity value of 1.63 kJ/kg.K for a hemp concrete with density equal to 508 kg/m^3. The results were obtained using a novel measurement method on 900x900x30 mm^3 samples. The wide range of hemp concrete (HC) composites and existing experimental techniques are reflected in the discrepancy of available literature data. The thermal diffusivity values of HC are in the range 0.14 – 0.40 mm^2/s [11,110–113]. The reported values of HC thermal diffusivity are relatively lower than those of other common building materials. Fig. 10 shows the evolution of thermal diffusivity of HC compared to other standard building materials. It can be seen that the thermal diffusivity of hemp concrete remains low even near free saturation humidity values. The diffusivity of HC is ~ 5.3 times lower than that of mineral wool (0.04 W/mK) and 2.6 times lower than that of bricks. The values reported by Gourlay et al. [100] vary in the range ~ 0.33-0.65 mm^2/s and remain higher that those reported thus far in literature [11,110–113]. The actual discrepancy of thermal diffusivity literature values (data boundary shown in Fig. 10) impedes thorough integrative data analysis.

Insert Figure 10. Double column (Width 180 mm)

6. Hygroscopic behaviour of bio – based building materials

Bio-based building materials in general and hemp concrete are porous materials with a high ratio of open porosity. This particularity confers them with special hygroscopic behaviour. In fact, hemp concrete can adsorb large amounts of water vapour at increasing relative humidity. The adsorbed water vapour condenses in smaller pores and adhere on their inner surfaces. Inversely, in low relative humidity conditions, they release the adsorbed water vapour. These are absorption / desorption phenomena which consist in mass transport depending on water vapour permeability of the material that characterizes its ability to exchange moisture under a water vapour gradient at a steady state. This hygroscopic behaviour influences the thermal properties of bio-based building materials [6].

6.1. Pore structure and sorption – desorption.

The porous structure and water vapour sorption of hemp concretes have been extensively characterized by Collet et al. [75] using mercury intrusion porosimetry (MIP) and sorption techniques. The reported results for a hemp concrete of 76.5 % total porosity (70.6 % open porosity) and a unit weight of 440 kg/m^3, display a mono - modal pore size distribution with a peak diameter of 1 micron and a predominance of macropores (Φ >0.05 microns) representing ~ 94% of the mercury intrusive volume. The results show an intrusion / extrusion hysteresis which was attributed to the 'ink bottle' and 'contact angle' effects [75]. The hysteresis phenomena should be taken into account for precise hygrothermal behaviour modelling of hemp concrete [114].

To study the water vapour absorption kinetics of BBBMs, Rahim et al. [115] evaluated the moisture intake for hemp and rape straw concretes. The reported kinetics results have shown that adsorption phenomena are extremely slow with hemp and straw-lime concretes taking more than 350 and 200 days respectively to achieve equilibrium at 95% rh from 81% rh. The slowness of LHC sorption was reported for an equilibrium time of ~ 250 days at 97% rh after stabilization at

81% rh corroborating aforementioned pace reported by Collet-Foucault [5]. This long time for measurement presents limitations in terms of cost and risks associated with mold development during testing. Collet et al. [116] proposed a kinetic model to reduce adsorption measurement time to 20-40 days. The phenomena of adsorption and desorption are described using absorption – desorption isotherms coupled with the pore structure of materials. The obtained sorption curves are typical of meso and macro-porous materials with the observed hysteresis attributed to the 'ink-bottle' effect and the difference in contact angle at adsorption and desorption [5].

In some measurements of sorption, the initial points corresponding to the dry state at 0% rh differ in adsorption and desorption. This recorded increase in mass at dry state, was suggested to be a result of a chemical combination of some capillary pore water leading to the observed slight mass increase [13]. Contrary to the former phenomenon, other hemp concrete sorption isotherms have recorded perfect moisture recovery from adsorption back to desorption [110].

Temperature dependence of absorption isotherms (obtained from isosteric heat of adsorption and Clausius - Clapeyron equation) is associated to linear and instantaneous variations of relative humidity with temperature in a supposedly constant moisture content environment. A hygrometric coefficient of 0.5% rh/ °C at 50% rh was reported and a reduction in temperature associated with increasing relative humidity in the range 50 - 90% rh was confirmed [117]. Similar temperature dependence of sorption isotherms has been recorded where a decrease in temperature led to an increase in moisture content [118]. Tran-Le et al. discussed this temperature dependence behaviour of lime-hemp sorption and its influence on the hygrothermal behaviour using the experimental and coupled transient heat and mass transport modelling [119].

6.2. Moisture buffering potential of BBBMs

The moisture buffering potential of a material is measured using the moisture buffer value, MBV of the Nordtest. MBV relates the moisture exchange (equation 16) (uptake or release) from a unit surface under relative humidity gradient according to equation 17. This allows a classification of the moisture performance of materials in five classes for 8/16 h humid/dry testing period.

$$\begin{cases} G(t) = \int_0^t g(t)dt = bm \times \Delta p \times h(\alpha)\sqrt{t_p/\pi} \\ h(\alpha) = \frac{2}{\pi}\sum_{n=1}^{\infty} sin^2 (n\pi\alpha) / n^{3/2} \end{cases} \qquad \text{Eq.16}$$

$$MBV = \Delta m / A(RH_{in} - RH_{fin}) \qquad \text{Eq.17}$$

With G(t) the accumulated moisture exchange (kg/m^2) within time period t_p , g(t) the moisture flux over the surface, α the high relative humidity time period, b_m the moisture effusivity.
Collet et al. [116] reported MBV values of 2.14 and 2.15 g/m^2 % rh for sprayed and tamped hemp concrete respectively (430 kg/m^3 and 78.5 % total porosity) and 1.94 g/m^2 % rh for precast concrete (460 kg/m^3 and 72% total porosity). Literature suggests that taking into the account the dynamics of thermal and hygric exchanges of BBBMs can potentially enhance predictions of hygrothermal performances at scales higher than materials level. Several experimental and numerical investigations of hygrothermal performance of BBBMs walls highlighted positive effects on thermal performance and indoor comfort [120–126].These results were attributed to temperature dampening and relative humidity regulation abilities of BBBMs. Furthermore, a recent dynamic hygrothermal numerical simulation of hemp-lime wall assemblies by Alam [127], corroborated earlier statements [11]. These hygrothermal performances were reported in several other studies at the building scale [128–131].

7. Acoustic properties of bio–based building materials

Materials with a porous structure are capable of absorbing sounds through dissipation and conversion to heat of the incident waves within their pores [132]. Hemp concrete, having high porosity (70 - 90%), was investigated for its sound absorption properties through experimental and numerical modelling. Cérézo [6] carried out the earliest acoustic characterization of hemp concrete and recorded sound absorption values of 0.3-0.9 for the range of studied frequency values (100-2000 Hz). Transmission loss values of 43 dB for hemp concretes blocks (31 cm width and 700 kg/m^3) were reported [133]. Glé performed an extensive acoustic investigation of bio-materials reinforced with fibres and particles and developed numerical models inspired from porous materials transport phenomena [134].

In their investigations of the effects of hemp shiv size and binder type/content, density and manufacturing process on sound absorption and transmission loss of BBBMs, Glé et al. [95] found that for the same binder type, the influence of the aggregate size was negligible for all the absorption frequencies. On the other hand, the type of binder, degree of compaction and binder content were identified as principal parameters influencing sound absorption. Hemp-lime exhibitss higher sound absorption than hemp-cement due to matrix high porosities (50 -52% for binders for air and hydraulic lime respectively and 39.0% for quick natural cement). The degree of compaction has a more interesting double effect with higher compaction translating absorption peaks towards lower frequencies and decreasing their intensities at high frequencies (1200-2000 Hz) while increasing them at low frequencies (400-700 Hz). The influence of binders on multiscale properties of hemp concretes was conducted, and the acoustic performances of hemp-lime and hemp-cement composites (4 cm thick and 130 kg/m^3) were reported in [135]. The sound absorption of the composites was recorded at peak values of ~ 0.90-0.98 at 1250Hz. The composites exhibit higher absorption and transmission loss values than the shiv particles.

Hemp-lime composites made of different binders including calcic lime (CL90s), metakaolin (MK) and ground granulated blast furnace slag (GGBS) [136] showed different behaviour, confirming the effect of binder type on the acoustic performance of BBBMs. Glé et al. [137] observed a similar behaviour on lime-based binders and hydraulic binders. A single absorption peak at 450 Hz was observed with a generalized low absorption over the whole frequency range 400-2000 Hz reflecting the values observed for quick natural cement dense matrices [95]. Compared to un-rendered HLCs, the application of 1 mm thick hemp-lime render reduced the sound absorption by 1.5, 2.17 and 1.86 times for 500, 1000 and 2000 Hz frequencies respectively (binder of 80% CL90 + 20%GGBS + 0.5% methyl-cellulose for b/a 1, w/b 1.5). The acoustic properties of miscanthus-cement were studied in [32]. Like for hemp-lime, the recorded absorption coefficients were 0.6 for the frequency range of 1.0-1.25 kHz and 0.5 for 1.25-1.60 kHz, respectively for the volumetric ratios of miscanthus of 20% and 30%. The authors report a shift of the absorption peak to higher frequencies as the miscanthus ratio increases.

A comparative analysis of the hemp - lime and hemp - clay composites confirmed similar behaviour with regard to their profile of sound absorption and transmission loss [88]. In fact, the similitude of behaviour is a result of inter-particle pores structure. It was observed that for low density values (< 375kg/m^3), the absorption peak (0.6-1.0) appears within the frequency range of 700-1500 Hz for hemp-clay while it appears within the range of 600-2000 Hz for hemp-lime. Nevertheless, for the same unit weight, the transmission losses recorded for both composites were around 5 dB for all the frequency ranges. It was reported that the absorption frequency range decreases and peaks diminish in intensity for high density composites [138]. Fernea et al. [139] have studied the acoustic properties of hemp-cement composites and found the highest absorption peaks at 1000 Hz and 1500 Hz with values of 0.80 and 0.90 for shiv and fibres, respectively (b/a 2.0 and w/b 1.0). The lowest absorption coefficients reported were 0.50 and 0.65 in the 2000 – 2800 Hz frequency range for shiv and fibres, respectively. Hemp concrete show comparable transmission loss values to those of cellular concrete blocks, (43 and 52 dB for hemp and cellular concrete respectively) and higher sound absorption coefficient (0.4-0.6 and 0.09-0.18 for hemp and cellular concrete respectively) with 1.50 times less energy consumption and global warming potential (- 14 to -35 and 52.3 for hemp and cellular concrete respectively) [140].

Literature reports values of acoustic absorption coefficients in the range 0.3-0.9 for hemp concrete made of a variety of binders. The binder content is the most relevant parameter that affects the acoustic performance of BBBMs. In fact, the increase of binder volume reduces the open porosity and hence the permeability of composites. The analysis of absorption profiles in [6,134] shows that an increase of binder content results in a reduction of the absorption amplitude, a narrowing of the absorption bands and their shifting towards low frequencies. Absorption coefficients can be analysed per octave to reduce local variations of absorption profiles, and hence allowing a critical comparison amongst different materials and wall systems as shown in Fig. 11. Hemp-concrete (HC) has a high open porosity (~70%) [5], which allows high air permeability and thus, it exhibits relatively high acoustic absorption coefficients compared to common materials used in buildings (α<0.15)[141]. HC and aerated autoclaved concrete (AAC) have comparable total porosity values in the range 70-90%. Though, that of hemp concrete is ~90% open porosity as opposed to 38.6 – 47.3% for AAC [142]. Therefore, the acoustic absorption of AAC is < 0.4, which is less than that of most hemp concretes. Optimistically, the acoustic absorption performance of hemp concrete can be compared with acoustic systems used in buildings such as mineral fibre and perforated panels. Literature data (Fig. 11) show that the acoustic absorption of 200 mm hemp concrete can be higher than that of 14% perforated panel - 25 mm cavity containing mineral fibre (α=0.5-0.8), and in some cases, near that of a 50 mm mineral fibre (α=0.79-0.9). However, the application of rendering/coating on the surface of hemp concrete can significantly reduce the air permeability and hence the acoustic absorption. Kinnane et al. [136] reported reductions of 50% of the absorption by the application of 10 mm rendering on hemp-lime.

Insert Figure 11. Double column / width: 180 mm

8. Life cycle analysis of bio-based building materials

The analysis of the environmental (energy and carbon) flows of the aggregates and binders is the precursor to the study of environmental impact of the bio-composites. Life cycle assessment of hemp cultivation and use of hemp-based insulating materials in buildings was covered in [143] considering the impact of production practices on environment [144]. Results report values of production energy requirements of 11 400 MJ/ha (compared to 18 100MJ/ha for wheat and 23 000MJ//ha for maize).The earliest UK environmental analysis / LCA of bio - based constructions concerned straw bales and carbon reduction potential of 61.0% was reported for a 60-years life building [145]; confirming the de-carbonation or ‘carbon-sink’ potential of bio-based buildings.

Life cycle assessment of sprayed hemp concrete wall (considering wall thickness and wall coating) was performed and results reported in [2]. The authors set the functional unit to meet thermal regulations of maximal heat transmittance U of 0.36 W/m^{2}K and the lifespan of 100 years with coating renewal at 33 and 50 years respectively for outdoor (2 cm sand-lime) and indoor (1 cm hemp-lime). The scenarios considered nine environmental indicators and the results have shown that the highest contribution to all indicators at 49.33-89.54% is attributable to raw materials production. The operational phase of the building recorded the lowest impact, with 5-15 % of the total impact (attributed to the refurbishment of coatings). Components of the wall contributed to the impacts in different proportions with the largest contribution attributed to binders (68% of water consumption, 49% of primary energy demand and 47% of the air pollution) for overall binder weight by weight content of 26.65 (w/w%). The overall impact related to the climate change is estimated at 0.21 kg CO_2eq and net emissions at –0.016 kg CO_2eq (considering the use phase evaluated at -0.20 kg CO_2eq.)

A comparative life cycle of hemp-lime wall constructions in the UK was conducted considering a functional unit (FU) of a timber framed wall (1.0 m^2 x 300 mm) using SimaPro with the guidelines of ISO 14040, UK PAS 2050 for a period of 100 years [1]. The authors reported a high contribution to GHG by lime (77.4%) compared to hemp hurds (12.4%). The total reported GHG emissions amount to -36.08 CO2eq/FU and 46.63 kg CO_2eq/FU respectively with and without considering hemp and lime CO_2 absorption/sequestration. Arrigoni et al. [146] studied the life cycle of hemp-based materials emphasizing on the role of carbonation of hemp concrete blocks. The authors found that considering complete carbonation of the hemp concrete during the use phase was unrealistic, and concluded that the negative GHG balance observed was due to the biogenic CO_2 uptake estimated at 58.0 kgCO_2eq (representing ~ 84% of all the CO_2 uptake at 240 days of curing). On the other hand, Berge [147] reported that 90% of the lime-production CO_2 can be re-carbonated (0.63 tonnes of CO_2/ ton of lime). Arrigoni et al. [146] reported a net GHG balance of - 12.09 kgCO_2eq/FU. The authors estimated a net balance of - 26.01 kgCO2eq/FU considering full lime carbonation. Ip and Miller [1] reported carbon storage values of -36.08 kgCO2eq/FU for hemp concrete, corroborating figures reported by Boutin et al.: -35.53 kgCO_2eq/FU [140].

9. Resources availability for bio-based materials in South West England: an opportunity for miscanthus ?

Miscanthus giganteus (elephant grass) is a perennial hybrid of miscanthus sacchariflorus and sinensis originating from South – East Asia. Introduced in Europe in the 1930’s, it can grow on barren marginal contaminated land with long-term harvestable yield of 13 dry tonnes per hectare per year [148]. It was introduced in the UK for use in the heat and electric energy production in power stations, combined heat and power units or heating systems. According to the Department of Environmental Food and Rural Affairs (DEFRA), 55 000 tonnes were used in UK power stations to produce electricity in 2016/17 (around ¾ of all miscanthus produced in England in 2017). Industrial and non-food crops (energy crops) agricultural land surface was estimated at 2.0% of all the arable land with 129 000 hectares in 2017, and this could be potential source for bio-based materials, in addition to agricultural wastes/co-products in the UK. Miscanthus represented 7 366 hectares (ha) in 2017 (0.1% of the total arable land in England) with a slight decrease compared to the highest developed land in 2009 (9 213 ha) with a production of 74 – 110 (lower and upper estimates) thousands of oven dried tonnes. The UK biomass strategy estimates that up to 350 000 ha could be grown in the UK with no impact on the food production (Agrikinetics).

Crops absorb carbon through CO_2 to biomass conversion and their contribution is considerable. Hemp (cannabis sativa) can absorb 15 tonnes of CO_2 per hectare. Miscanthus x giganteus has a sequestration rate of 1.96 ± 0.82 Mg C ha^{-1} $year^{-1}$ for over six years (~ 7.19 ± 3.00 tonnes of CO_2 ha^{-1} $year^{-1}$) [149]. These crops can be used to produce carbon sinks of bio-based materials. Nonetheless, the estimation of GHG mitigation of crops remains a relatively complex subject due to the interaction of bio-climatic and soils conditions in addition to the dynamics of carbon capture, exchange, and storage in the soil-air-plant system. Mining associated activities in the South West England (Devon and Cornwall) have been thriving and are renowned historically for tin, copper and arsenic production since the Bronze Age [150]. The exploitation of numerous metalliferous mining sites in this region has led to heavy metals contaminations namely in water (Thallium) [151] and soils (Arsenic) [152]. On the other hand, several studies have pointed out the potential of Miscanthus for phytoremediation of heavy metals contaminated lands [153,154] and former mining sites [155]. These sites could be potentially reclaimed for the development of Miscanthus in the Devon and Cornwall.

Vegetal particles and fibres (hemp, sisal, jute, flax) have been applied in thermoplastic polymers reinforcement: polyethylene [156], polypropylene [157–159], and polyvinyl-chloride

[160], as well as thermosets reinforcement such as polyester [161] and epoxy resin [162]. A recent extensive review on phenolic polymers and their composites detailed the use of hemp, sisal, oil palm fibres, coir fibres, jute, banana, and cotton fibres in phenolic resin matrices [163]. The authors reported promising mechanical properties of composites with several potential applications in aircraft, transportation, and construction. The presence of a wide spectrum of potential applications, as well as their economic-environmental potentials, have revitalised interests in the development of bio-composites in both academia and industry. Some recent works on bio-fibres composites include Gheith et al. [164], Saba et al. [165,166], Asim et al. [167], Khan et al. [168], Hanan et al. [169], Sanjay et al. [170] and Pickering et al. [171]. Cement reinforcement using natural fibres has been summarized in a recent review covering the effects of fibre type and characteristics over fresh and hardened properties of the composites [172]. The use of miscanthus in construction industry is a novel application. Some recent research covered the use of saccharification by-products of miscanthus for cement reinforcement [51] and the influence of the chemical treatments on miscanthus stems [173,174]. Chen et al. [32] investigated the acoustic performance of cement-miscanthus lightweight concrete and Lv et al. [175] evaluated the influence of miscanthus ash on autogenous shrinkage of Portland pastes and reported results encourage both the incorporation of miscanthus aggregates in lightweight composites and the incorporation of miscanthus ash in cement. Miscanthus is a potential crop that is particularly interesting in the context of South West England. It constitutes a potential sustainable solution to barren lands, a possibility of regional carbon capture and storage, a prospective development of insulation materials for regional buildings considering actual energy directives.

10. Conclusions

Bio-based composite materials have multiple potential applications that range from mineral binders-based buildings insulating materials to organic binders-based composites for aircraft and transportation industries. The recent growing attention paid to sustainability and low-carbon built environment has spurred research on mechanical, thermal, and acoustic properties of these composites. The wide range of applications and associated manufacturing techniques has resulted in an ever-extensive literature. This paper attempts to cover the existing knowledge on vegetal fibre based composite materials from the chemical and microstructural aspects to the macro properties (mechanical, hygrothermal and acoustic properties) with an emphasis on mineral binder-based materials. A number of major findings from the reviewed literature can be listed:

- The basic chemical composition of lignocellulosic materials (polysaccharides) results in incompatibility problems related either to water absorption of hydrophilic groups or to the leakages of chemicals that interfere with the setting and hardening of mineral binders. Chemical, physical, and mixed treatment techniques were developed to address the compatibility of biomass aggregates and mineral/organic binders. The use of alkali solutions is the most widespread technique and allows the effective removal of hemicellulose and lignin, enhancement of mechanical and microstructural properties. However, the efficiency of those treatments varies in terms of water absorption reduction, increase of the surface area, fibre-matrix bonding, strength enhancement and highly depend on the nature of the vegetal fibre.

- Mechanical properties of BBBMs are extensively covered in the literature. The impact of compactness, i.e. density of samples on the uniaxial compressive strength, was critically examined. The ratio of mix constituents and manufacturing techniques play a significant role in the development of compressive strength of BBBM composites. In particular, the binder to aggregate ratio (b/a) is responsible for controlling the density and strength at constant compactness. The compaction and projection manufacturing processes result in preferential orientation of aggregates within the composites, resulting in anisotropic mechanical behaviour. In general, BBBMs have low compressive strength values in general (0.1-3.5N/mm^2) compared to lightweight concrete blocks (7-14 N/mm^2) and bricks. However, relatively high strength values can be achieved using high compaction stresses during the casting process. The shear resistance of BBBMs highlighted values of cohesion strength of 355 kPa (peak friction angle of 46°), suggesting the potential contribution in design of lighter structural timber frames.
- Thermal conductivity of BBBMs is lower (0.06-0.20 W/m.K) than that of common building materials (concrete blocks and autoclaved aerated concrete blocks) due to their high porosity (70-90%). However, the reported thermal conductivity values vary significantly depending on the composition of the mix, manufacturing techniques and water content of the composites. Relatively high thermal conductivity values were obtained for projected hemp concrete (~0.3-0.8 W/m.K) compared to tampered or compacted hemp concrete (<0.2 W/mK). BBBMs remain anisotropic composites due to both the manufacturing techniques and the shape aggregates.
- Transient thermal performance of BBBMs is less covered in literature even though a number of studies reported the increased transient thermal performance associated with the low thermal diffusivity of BBBMs (0.14-0.60 mm^2/s), owing to their high specific heat capacity (0.9-1.5 KJ/kg.K). The actual thermal performance regulations use thermal transmittance U-values to estimate performance of buildings. However, literature

revealed that dynamic thermal performance including the thermal capacitance of walls allow to suggest that the actual thermal performance of BBBMs is underrated.

- The reported data on acoustic performance of BBBMs highlight values of acoustic absorption coefficients in the range of 0.3 – 0.9 over the frequency zone 125 – 2000 Hz. In some cases, BBBMs can provide a performance comparable to that of the actual commercial acoustic panels. It should be considered that the acoustic performance relies on the availability of open porosity and air permeability. Therefore, the application of a rendering significantly reduces the acoustic absorption of BBBMs.
- The sustainability aspect of BBBMs is a highly discussed subject and advanced as a motivation for their development. However, literature data remains scarce to support the previous statement quantitatively. Existing data suggests carbon storage potential of 26.01 – 36.08 $kgCO_2eq./m^2$ for walls of 260 – 300 mm thickness. However, these values although indicative, remain case-specific and the environmental performance of BBBMs remains closely related to the local availability of bio-aggregates.

Although the existing literature covers effectively various aspects bio-based building materials, continued research on the chemical-microstructural and macro-properties is crucial to improve the understanding of these novel materials, and thus promote their widespread acceptance and use. Potential future research on the aspects of chemical-microstructural elements of BBBMs could include amongst others :

- The in-depth investigation of mineral binders and vegetal aggregates interactions focusing on the physical and chemical impacts of binder matrix on the vegetal aggregates on mid and long term, and vice versa.
- The effects of chemical and physical treatments on hardening reactions and mechanisms of binder matrices.
- The behaviour of vegetal aggregates in alkali activated binder matrix (chemical and morphological evolutions).

Considering macro-properties, a number of technical elements would ultimately revitalise the interest in the application of BBBMs at large scale by providing further information. These include:

- The study of combined effect of compaction and fibre size optimisation on strength and insulation (thermal and acoustic).
- The use of alkali-activated binder matrices and their effects on strength and insulation properties (thermal and acoustic).

- The long-term durability of BBBMs at the wall / building scale.

There is significant potential in reducing carbon footprint of the built environment using bio-based building materials. This context provides authentic opportunities for miscanthus crop growers in the South West of England, to add value to miscanthus products while addressing the actual environmental challenges. Continued research to address the identified research questions will thrust the acknowledgement of bio-based building materials from the construction industry and building regulating bodies, and bring about a widespread utilisation of bio-based building materials in the South West of England, and the UK in general.

Acknowledgement and funding:
This article is part of ongoing research at the College of Engineering, Mathematics and Physical Sciences of the University of Exeter in partnership with the BRE Centre in Innovation Construction Materials of the University of Bath. This project is supported by a NERC GW4+ Doctoral Training Partnership from the Natural Environment Research Council (NERC) and the National Productivity Investment Fund (NPIF) [NE/R011621/1]. The authors are thankful for the support and additional funding from CASE (Collaborative Awards in Science and Engineering) partners: Miscanthus Nursery Ltd and Agrikinetics Ltd.

References

[1] K. Ip, A. Miller, Life cycle greenhouse gas emissions of hemp–lime wall constructions in the UK, Resour. Conserv. Recycl. 69 (2012) 1–9. https://doi.org/10.1016/j.resconrec.2012.09.001.

[2] S. Pretot, F. Collet, C. Garnier, Life cycle assessment of a hemp concrete wall: Impact of thickness and coating, Build. Environ. 72 (2014) 223–231. https://doi.org/10.1016/j.buildenv.2013.11.010.

[3] M.S. McLaggan, Novel fire testing frameworks for Phase Change Materials and hemp-lime insulation, Ph.D. Thesis, University of Edinburgh, 2016. http://hdl.handle.net/1842/15896 (accessed June 23, 2020).

[4] G. Delannoy, Durabilité d'isolants à base de granulats végétaux, Thèse de doctorat, Université Paris-Est, 2018. https://tel.archives-ouvertes.fr/tel-02141189 (accessed June 23, 2020).

[5] F. Collet-Foucault, Caractérisation hydrique et thermique de matériaux de génie civil à faibles impacts environnementaux, Thèse de doctorat, INSA Rennes, 2004. http://www.theses.fr/2004ISAR0016 (accessed June 23, 2020).

[6] V. Cérézo, Propriétés mécaniques, thermiques et acoustiques d'un matériau à base de particules végétales : approche expérimentale et modélisation théorique, Thèse de doctorat, INSA Lyon, 2005. http://www.theses.fr/2005ISAL0037 (accessed June 23, 2020).

[7] V. Nozahic, Vers une nouvelle démarche de conception des bétons de végétaux lignocellulosiques basée sur la compréhension et l'amélioration de l'interface liant / végétal : application à des granulats de chenevotte et de tige de tournesol associés à un liant

ponce / chaux, Thèse de doctorat, Université Clermont-Ferrand 2, 2012. http://www.theses.fr/2012CLF22265 (accessed June 23, 2020).
[8] D. Sedan, Etude des interactions physico-chimiques aux interfaces fibres de chanvre/ciment : influence sur les propriétés mécaniques du composite, Thèse de doctorat, Université de Limoges, 2007. http://www.theses.fr/2007LIMO4055 (accessed June 23, 2020).
[9] J. Chamoin, Optimisation des propriétés (physiques, mécaniques et hydriques) de bétons de chanvre par la maîtrise de la formulation, Thèse de doctorat, INSA Rennes, 2013. http://www.theses.fr/2013ISAR0016 (accessed June 23, 2020).
[10] T.T. Nguyen, Contribution à l'étude de la formulation et du procédé de fabrication d'éléments de construction en béton de chanvre, Thèse de doctorat, Université de Bretagne Sud, 2010. https://tel.archives-ouvertes.fr/tel-01017510/document.
[11] A. Evrard, Transient hygrothermal behaviour of Lime-Hemp Materials, Ph.D. Thesis, UCL - Université Catholique de Louvain, 2008. https://dial.uclouvain.be/pr/boreal/object/boreal:19675 (accessed June 23, 2020).
[12] A.D. Tran Le, Etude des transferts hygrothermiques dans le béton de chanvre et leur application au bâtiment, Thèse de doctorat, Université de Reims, 2010. https://www.theses.fr/2010REIMS012 (accessed June 23, 2020).
[13] E. Gourlay, Caractérisation expérimentale des propriétés mécaniques et hygrothermiques du béton de chanvre. Détermination de l'impact des matières premières et de la méthode de mise en oeuvre, Thèse de doctorat, ENTPE, 2014.
[14] G. Costantine, Etude et optimisation des performances énergétiques d'une enveloppe en béton de chanvre pour le bâtiment, Thèse de doctorat, Université de Reims Champagne-Ardenne, 2018. http://www.theses.fr/2018REIMS015 (accessed June 23, 2020).
[15] E. Latif, Hygrothermal performance of hemp based thermal insulation materials in the UK, Ph.D. Thesis, University of East London, 2013. https://doi.org/10.15123/PUB.3454.
[16] M. Chabannes, E. Garcia-Diaz, L. Clerc, J.-C. Bénézet, F. Becquart, Lime Hemp and Rice Husk-Based Concretes for Building Envelopes, Springer International Publishing, 2018. https://doi.org/10.1007/978-3-319-67660-9.
[17] S. Amziane, F. Collet, eds., Bio-aggregates Based Building Materials : State-of-the-Art Report of the RILEM Technical Committee 236-BBM, Springer Netherlands, 2017. https://doi.org/10.1007/978-94-024-1031-0.
[18] E. Chabi, A. Lecomte, E.C. Adjovi, A. Dieye, A. Merlin, Mix design method for plant aggregates concrete: Example of the rice husk, Constr. Build. Mater. 174 (2018) 233–243. https://doi.org/10.1016/j.conbuildmat.2018.04.097.
[19] M.P. Sáez-Pérez, M. Brümmer, J.A. Durán-Suárez, A review of the factors affecting the properties and performance of hemp aggregate concretes, J. Build. Eng. 31 (2020) 101323. https://doi.org/10.1016/j.jobe.2020.101323.
[20] L.P. Ramos, The chemistry involved in the steam treatment of lignocellulosic materials, Quím. Nova. 26 (2003) 863–871. https://doi.org/10.1590/S0100-40422003000600015.
[21] M. Lewin, Handbook of Fiber Chemistry, CRC Press, 2006. https://doi.org/10.1201/9781420015270.
[22] M.R. Vignon, C. Garcia-Jaldon, D. Dupeyre, Steam explosion of woody hemp chènevotte, Int. J. Biol. Macromol. 17 (1995) 395–404. https://doi.org/10.1016/0141-8130(96)81852-6.
[23] A.B. Thomsen, S.K. Rasmussen, V. Bohn, K.V. Nielsen, A. Thygesen, Hemp raw materials: The effect of cultivar, growth conditions and pretreatment on the chemical composition of the fibres, Risø National Laboratory, 2005. https://orbit.dtu.dk/en/publications/hemp-raw-materials-the-effect-of-cultivar-growth-conditions-and-p (accessed June 23, 2020).
[24] Y. Diquélou, E. Gourlay, L. Arnaud, B. Kurek, Impact of hemp shiv on cement setting and hardening: Influence of the extracted components from the aggregates and study of the

interfaces with the inorganic matrix, Cem. Concr. Compos. 55 (2015) 112–121. https://doi.org/10.1016/j.cemconcomp.2014.09.004.

[25] M. Viel, F. Collet, C. Lanos, Chemical and multi-physical characterization of agro-resources’ by-product as a possible raw building material, Ind. Crops Prod. 120 (2018) 214–237. https://doi.org/10.1016/j.indcrop.2018.04.025.

[26] E.M. Hodgson, D.J. Nowakowski, I. Shield, A. Riche, A.V. Bridgwater, J.C. Clifton-Brown, I.S. Donnison, Variation in miscanthus chemical composition and implications for conversion by pyrolysis and thermo-chemical bio-refining for fuels and chemicals, Bioresour. Technol. 102 (2011) 3411–3418. https://doi.org/10.1016/j.biortech.2010.10.017.

[27] D. Dai, M. Fan, Characteristic and performance of elementary hemp fibre, Mater. Sci. Appl. 01 (2010) 336. https://doi.org/10.4236/msa.2010.16049.

[28] M. Chabannes, E. Garcia-Diaz, L. Clerc, J.-C. Bénézet, Effect of curing conditions and Ca(OH)2-treated aggregates on mechanical properties of rice husk and hemp concretes using a lime-based binder, Constr. Build. Mater. 102 (2016) 821–833. https://doi.org/10.1016/j.conbuildmat.2015.10.206.

[29] J. Keckes, I. Burgert, K. Frühmann, M. Müller, K. Kölln, M. Hamilton, M. Burghammer, S.V. Roth, S. Stanzl-Tschegg, P. Fratzl, Cell-wall recovery after irreversible deformation of wood, Nat. Mater. 2 (2003) 810–813. https://doi.org/10.1038/nmat1019.

[30] P. Fratzl, R. Weinkamer, Nature’s hierarchical materials, Prog. Mater. Sci. 52 (2007) 1263–1334. https://doi.org/10.1016/j.pmatsci.2007.06.001.

[31] Y. Jiang, R. Lawrence, M. Ansell, A. Hussain, Cell wall microstructure, pore size distribution and absolute density of hemp shiv: Microstructure, porosity and absolute density, R. Soc. Open Sci. 5 (2018) 1–15. https://doi.org/10.1098/rsos.171945.

[32] Y. Chen, Q.L. Yu, H.J.H. Brouwers, Acoustic performance and microstructural analysis of bio-based lightweight concrete containing miscanthus, Constr. Build. Mater. 157 (2017) 839–851. https://doi.org/10.1016/j.conbuildmat.2017.09.161.

[33] B. Mazhoud, Elaboration et caractérisation mécanique, hygrique et thermique de composites bio-sourcés, These de doctorat, Rennes, INSA, 2017. http://www.theses.fr/2017ISAR0024 (accessed June 23, 2020).

[34] D. Sedan, C. Pagnoux, T. Chotard, A. Smith, D. Lejolly, V. Gloaguen, P. Krausz, Effect of calcium rich and alkaline solutions on the chemical behaviour of hemp fibres, J. Mater. Sci. 42 (2007) 9336–9342. https://doi.org/10.1007/s10853-007-1903-4.

[35] M. Bishop, A.R. Barron, Cement hydration inhibition with sucrose, tartaric acid, and lignosulfonate: analytical and spectroscopic study, Ind. Eng. Chem. Res. 45 (2006) 7042–7049. https://doi.org/10.1021/ie060806t.

[36] A. Arizzi, G. Cultrone, M. Brümmer, H. Viles, A chemical, morphological and mineralogical study on the interaction between hemp hurds and aerial and natural hydraulic lime particles: Implications for mortar manufacturing, Constr. Build. Mater. 75 (2015) 375–384. https://doi.org/10.1016/j.conbuildmat.2014.11.026.

[37] D.P. Miller, Wood-cement composites: Interactions of wood components with Portland cement., (1989) 187.

[38] K. Bilba, M.-A. Arsene, A. Ouensanga, Sugar cane bagasse fibre reinforced cement composites. Part I. Influence of the botanical components of bagasse on the setting of bagasse/cement composite, Cem. Concr. Compos. 25 (2003) 91–96. https://doi.org/10.1016/S0958-9465(02)00003-3.

[39] A. Govin, A. Peschard, E. Fredon, R. Guyonnet, New insights into wood and cement interaction, Holzforschung. 59 (2005) 330–335. https://doi.org/10.1515/HF.2005.054.

[40] A. Govin, A. Peschard, R. Guyonnet, Modification of cement hydration at early ages by natural and heated wood, Cem. Concr. Compos. 28 (2006) 12–20. https://doi.org/10.1016/j.cemconcomp.2005.09.002.

[41] T.M. Dinh, Contribution au développement de béton de chanvre préfabriqué utilisant un liant pouzzolanique innovant, Thèse de doctorat, Université Toulouse 3, 2014. http://www.theses.fr/2014TOU30078 (accessed June 23, 2020).
[42] P. Coatanlem, R. Jauberthie, F. Rendell, Lightweight wood chipping concrete durability, Constr. Build. Mater. 20 (2006) 776–781. https://doi.org/10.1016/j.conbuildmat.2005.01.057.
[43] A.O. Olorunnisola, Effects of husk particle size and calcium chloride on strength and sorption properties of coconut husk–cement composites, Ind. Crops Prod. 29 (2009) 495–501. https://doi.org/10.1016/j.indcrop.2008.09.009.
[44] M. Khazma, N. El Hajj, A. Goullieux, R.M. Dheilly, M. Queneudec, Influence of sucrose addition on the performance of a lignocellulosic composite with a cementious matrix, Compos. Part Appl. Sci. Manuf. 39 (2008) 1901–1908. https://doi.org/10.1016/j.compositesa.2008.09.014.
[45] M. Bederina, M. Gotteicha, B. Belhadj, R.M. Dheily, M.M. Khenfer, M. Queneudec, Drying shrinkage studies of wood sand concrete – Effect of different wood treatments, Constr. Build. Mater. 36 (2012) 1066–1075. https://doi.org/10.1016/j.conbuildmat.2012.06.010.
[46] M. Le Troëdec, C.S. Peyratout, A. Smith, T. Chotard, Influence of various chemical treatments on the interactions between hemp fibres and a lime matrix, J. Eur. Ceram. Soc. 29 (2009) 1861–1868. https://doi.org/10.1016/j.jeurceramsoc.2008.11.016.
[47] R.D. Tolêdo Filho, K. Ghavami, G.L. England, K. Scrivener, Development of vegetable fibre–mortar composites of improved durability, Cem. Concr. Compos. 25 (2003) 185–196. https://doi.org/10.1016/S0958-9465(02)00018-5.
[48] A. Hussain, J. Calabria-Holley, M. Lawrence, Y. Jiang, Hygrothermal and mechanical characterisation of novel hemp shiv based thermal insulation composites, Constr. Build. Mater. 212 (2019) 561–568. https://doi.org/10.1016/j.conbuildmat.2019.04.029.
[49] N.A. Ramlee, M. Jawaid, E.S. Zainudin, S.A.K. Yamani, Modification of Oil Palm Empty Fruit Bunch and Sugarcane Bagasse Biomass as Potential Reinforcement for Composites Panel and Thermal Insulation Materials, J. Bionic Eng. 16 (2019) 175–188. https://doi.org/10.1007/s42235-019-0016-5.
[50] M. Asim, M. Jawaid, K. Abdan, M.R. Ishak, Effect of Alkali and Silane Treatments on Mechanical and Fibre-matrix Bond Strength of Kenaf and Pineapple Leaf Fibres, J. Bionic Eng. 13 (2016) 426–435. https://doi.org/10.1016/S1672-6529(16)60315-3.
[51] T. Le Ngoc Huyen, M. Queneudec T'Kint, C. Remond, B. Chabbert, R.-M. Dheilly, Saccharification of Miscanthus x giganteus, incorporation of lignocellulosic by-product in cementitious matrix, C. R. Biol. 334 (2011) 837.e1-837.e11. https://doi.org/10.1016/j.crvi.2011.07.008.
[52] X. Zhang, F. Wang, L.M. Keer, Influence of surface modification on the microstructure and thermo-mechanical properties of bamboo fibers, Materials. 8 (2015) 6597–6608. https://doi.org/10.3390/ma8105327.
[53] T.A. Negawo, Y. Polat, F.N. Buyuknalcaci, A. Kilic, N. Saba, M. Jawaid, Mechanical, morphological, structural and dynamic mechanical properties of alkali treated Ensete stem fibers reinforced unsaturated polyester composites, Compos. Struct. 207 (2019) 589–597. https://doi.org/10.1016/j.compstruct.2018.09.043.
[54] L.T.T. Vo, P. Navard, Treatments of plant biomass for cementitious building materials – A review, Constr. Build. Mater. 121 (2016) 161–176. https://doi.org/10.1016/j.conbuildmat.2016.05.125.
[55] K. Korniejenko, E. Frączek, E. Pytlak, M. Adamski, Mechanical properties of geopolymer composites reinforced with natural fibers, Procedia Eng. 151 (2016) 388–393. https://doi.org/10.1016/j.proeng.2016.07.395.

[56] J. Page, M. Sonebi, S. Amziane, Design and multi-physical properties of a new hybrid hemp-flax composite material, Constr. Build. Mater. 139 (2017) 502–512. https://doi.org/10.1016/j.conbuildmat.2016.12.037.

[57] R. Chen, S. Ahmari, L. Zhang, Utilization of sweet sorghum fiber to reinforce fly ash-based geopolymer, J. Mater. Sci. 49 (2014) 2548–2558. https://doi.org/10.1007/s10853-013-7950-0.

[58] P. Duan, C. Yan, W. Zhou, W. Luo, Fresh properties, mechanical strength and microstructure of fly ash geopolymer paste reinforced with sawdust, Constr. Build. Mater. 111 (2016) 600–610. https://doi.org/10.1016/j.conbuildmat.2016.02.091.

[59] S.N. Sarmin, J. Welling, Lightweight geopolymer wood composite synthesized from alkali-activated fly ash and metakaolin, J. Teknol. 78 (2016). https://doi.org/10.11113/.v78.8734.

[60] V.K. Doko, E.C. Adjovi, G.G. Aisse, C. Delisee, P. Galimard, Etude comparative de deux composites à matrice cimentaire renforcée par des fibres de borassus aethiopum mart. et des balles de riz, Ann. Sci. Agron. 17 (2013) 193–203. https://doi.org/10.4314/asab.v17i2.

[61] A. Akkaoui, Bétons de granulats de bois : étude expérimentale et théorique des propriétés thermo-hydro-mécaniques par des approches multi-échelles, Thèse de doctorat, Université Paris-Est, 2014. https://pastel.archives-ouvertes.fr/tel-01162671 (accessed June 23, 2020).

[62] F. française du bâtiment, Y. Association Construire en chanvre (Saint-Valérien, Construire en chanvre: règles professionnelles d’exécution, SEBTP, 2012.

[63] V. Nozahic, S. Amziane, G. Torrent, K. Saïdi, H. De Baynast, Design of green concrete made of plant-derived aggregates and a pumice–lime binder, Cem. Concr. Compos. 34 (2012) 231–241. https://doi.org/10.1016/j.cemconcomp.2011.09.002.

[64] P. Tronet, T. Lecompte, V. Picandet, C. Baley, Study of lime hemp composite precasting by compaction of fresh mix — An instrumented die to measure friction and stress state, Powder Technol. 258 (2014) 285–296. https://doi.org/10.1016/j.powtec.2014.03.002.

[65] L. Arnaud, E. Gourlay, Experimental study of parameters influencing mechanical properties of hemp concretes, Constr. Build. Mater. 28 (2012) 50–56. https://doi.org/10.1016/j.conbuildmat.2011.07.052.

[66] J. Williams, Modelling of a particle orientation in bio-based aggregate concretes, Ph.D. Thesis, University of Bath, 2017. https://researchportal.bath.ac.uk/en/studentthesis/modelling-of-a-particle-orientation-in-biobased-aggregate-concretes(850fe866-749d-4b89-8992-58e04f172bbf).html (accessed June 23, 2020).

[67] E.A.J. Hirst, Characterisation of hemp-lime as a composite building material, Ph.D. Thesis, University of Bath, 2013. https://researchportal.bath.ac.uk/en/studentthesis/characterisation-of-hempline-as-a-composite-building-material(8c88ff93-4601-44df-a553-9437f4e27aba).html (accessed June 23, 2020).

[68] P. Strandberg, Hemp concretes : mechanical properties using both shives and fibres, Ph.D. Thesis, Sveriges Lantbruksuniversitet, 2008. https://portal.research.lu.se/portal/en/publications/hemp-concretes--mechanical-properties-using-both-shives-and-fibres(22ac9b48-d2da-4052-8db4-78b596414fb5).html (accessed June 23, 2020).

[69] S. Elfordy, F. Lucas, F. Tancret, Y. Scudeller, L. Goudet, Mechanical and thermal properties of lime and hemp concrete (“hempcrete”) manufactured by a projection process, Constr. Build. Mater. 22 (2008) 2116–2123. https://doi.org/10.1016/j.conbuildmat.2007.07.016.

[70] T.T. Nguyen, V. Picandet, S. Amziane, C. Baley, Optimisation de l’usage du béton de chanvre dans la conception d’un éco-matériau pour le génie civil, Rev. Compos. Matér. Avancés. 18 (2008) 227.

[71] S. Kioy, Lime-hemp composites: Compressive strength and resistance to fungal attacks, Master Thesis, University of Bath, 2005.

[72] A. Kashtanjeva, M. Sonebi, S. Amziane, Investigation of the mechanical performance and drying shrinkage of hemp concrete, Acad. J. Civ. Eng. 33 (2015) 309–315. https://doi.org/10.26168/icbbm2015.47.

[73] P. Tronet, T. Lecompte, V. Picandet, C. Baley, Study of lime hemp concrete (LHC) – Mix design, casting process and mechanical behaviour, Cem. Concr. Compos. 67 (2016) 60–72. https://doi.org/10.1016/j.cemconcomp.2015.12.004.

[74] A. Youssef, V. Picandet, T. Lecompte, N. Challamel, Comportement du béton de chanvre en compression simple et cisaillement, in: Rencontres Univ. Génie Civ., Bayonne, France, 2015. https://hal.archives-ouvertes.fr/hal-01167596 (accessed June 23, 2020).

[75] F. Collet, M. Bart, L. Serres, J. Miriel, Porous structure and water vapour sorption of hemp-based materials, Constr. Build. Mater. 22 (2008) 1271–1280. https://doi.org/10.1016/j.conbuildmat.2007.01.018.

[76] E. Hirst, P. Walker, K. Paine, T. Yates, Characterisation of low density hemp-lime composite building materials under compression loading, in: 2010. https://researchportal.bath.ac.uk/en/publications/characterisation-of-low-density-hemp-lime-composite-building-mate (accessed June 23, 2020).

[77] R. Walker, S. Pavia, R. Mitchell, Mechanical properties and durability of hemp-lime concretes, Constr. Build. Mater. 61 (2014) 340–348. https://doi.org/10.1016/j.conbuildmat.2014.02.065.

[78] S. Pavia, R. Walker, J. McGinn, Effect of testing variables on the hydration and compressive strength of lime hemp concrete, Acad. J. Civ. Eng. 33 (2015) 635–640. https://doi.org/10.26168/icbbm2015.98.

[79] N. Stevulova, L. Kidalova, J. Junak, J. Cigasova, E. Terpakova, Effect of hemp shive sizes on mechanical properties of lightweight fibrous composites, Procedia Eng. 42 (2012) 496–500. https://doi.org/10.1016/j.proeng.2012.07.441.

[80] C. Magniont, G. Escadeillas, M. Coutand, C. Oms-Multon, Use of plant aggregates in building ecomaterials, Eur. J. Environ. Civ. Eng. 16 (2012) s17–s33. https://doi.org/10.1080/19648189.2012.682452.

[81] S. Pavia, R. Walker, Impact of water retainers in the strength, drying and setting of lime hemp concrete, in: 2012. http://www.tara.tcd.ie/handle/2262/66463 (accessed June 23, 2020).

[82] M. Sinka, L. Radina, G. Sahmenko, A. Korjakins, D. Bajare, Enhancement of lime-hemp concrete properties using different manufacturing technologies, Acad. J. Civ. Eng. 33 (2015) 301–308. https://doi.org/10.26168/icbbm2015.46.

[83] S. Amziane, V. Nozahic, M. Sonebi, Design of mechanically enhanced concrete using hemp shiv, Acad. J. Civ. Eng. 33 (2015) 422–426. https://doi.org/10.26168/icbbm2015.65.

[84] G. Balčiūnas, S. Vėjelis, S. Vaitkus, A. Kairytė, Physical Properties and Structure of Composite Made by Using Hemp Hurds and Different Binding Materials, Procedia Eng. 57 (2013) 159–166. https://doi.org/10.1016/j.proeng.2013.04.023.

[85] C. Niyigena, Variabilité des performances de bétons de chanvre en fonction des caractéristiques de la chènevotte produite en Auvergne, These de doctorat, Clermont-Ferrand 2, 2016. http://www.theses.fr/2016CLF22700 (accessed June 23, 2020).

[86] S. Pavia, R. Walker, An assessment of some physical properties of lime-hemp concrete, in: 2010. http://www.tara.tcd.ie/handle/2262/57402 (accessed June 23, 2020).

[87] J. Williams, M. Lawrence, P. Walker, The influence of constituents on the properties of the bio-aggregate composite hemp-lime, Constr. Build. Mater. 159 (2018) 9–17. https://doi.org/10.1016/j.conbuildmat.2017.10.109.

[88] P. Munoz, D. Pipet, Plant-Based Concretes in Structures: Structural Aspect – Addition of a Wooden Support to Absorb the Strain, in: Bio-Aggreg.-Based Build. Mater., John Wiley & Sons, Ltd, 2013: pp. 267–288. https://doi.org/10.1002/9781118576809.ch8.

[89] C.D. Gross, Structural enhancement of timber framing using hemp-lime, Ph.D. Thesis, University of Bath, 2013. https://researchportal.bath.ac.uk/en/studentthesis/structural-enhancement-of-timber-framing-using-hemplime(62ff92df-ff94-46b2-b56f-f13ff1f7665c).html (accessed June 23, 2020).

[90] C. Gross, P. Walker, Racking performance of timber studwork and hemp-lime walling, Constr. Build. Mater. 66 (2014) 429–435. https://doi.org/10.1016/j.conbuildmat.2014.05.054.

[91] A. Mukherjee, C. MacDougall, Structural benefits of hempcrete infill in timber stud walls, Int. J. Sustain. Build. Technol. Urban Dev. 4 (2013) 295–305. https://doi.org/10.1080/2093761X.2013.834280.

[92] M. Chabannes, F. Becquart, E. Garcia-Diaz, N.-E. Abriak, L. Clerc, Experimental investigation of the shear behaviour of hemp and rice husk-based concretes using triaxial compression, Constr. Build. Mater. 143 (2017) 621–632. https://doi.org/10.1016/j.conbuildmat.2017.03.148.

[93] A. Youssef, Prise en compte des apports mécaniques du béton de chanvre pour le calcul de structure bois/béton de chanvre et métal/béton de chanvre, Thèse de doctorat, Université Lorient, 2017. https://www.theses.fr/2017LORIS431 (accessed June 23, 2020).

[94] A. Shea, M. Lawrence, P. Walker, Hygrothermal performance of an experimental hemp–lime building, Constr. Build. Mater. 36 (2012) 270–275. https://doi.org/10.1016/j.conbuildmat.2012.04.123.

[95] P. Glé, E. Gourdon, L. Arnaud, Acoustical properties of materials made of vegetable particles with several scales of porosity, Appl. Acoust. 72 (2011) 249–259. https://doi.org/10.1016/j.apacoust.2010.11.003.

[96] T. w Clyne, I. o Golosnoy, J. c Tan, A. e Markaki, Porous materials for thermal management under extreme conditions, Philos. Trans. R. Soc. Math. Phys. Eng. Sci. 364 (2006) 125–146. https://doi.org/10.1098/rsta.2005.1682.

[97] F. Collet, S. Pretot, Thermal conductivity of hemp concretes: Variation with formulation, density and water content, Constr. Build. Mater. 65 (2014) 612–619. https://doi.org/10.1016/j.conbuildmat.2014.05.039.

[98] A.D. Tran-Le, S.-T. Nguyen, T. Langlet, A novel anisotropic analytical model for effective thermal conductivity tensor of dry lime-hemp concrete with preferred spatial distributions, Energy Build. 182 (2019) 75–87. https://doi.org/10.1016/j.enbuild.2018.09.043.

[99] D. Samri, Analyse physique et caractérisation hygrothermique des matériaux de construction, Thèse de doctorat, INSA Lyon, 2008. https://www.theses.fr/2008ISAL0067 (accessed June 23, 2020).

[100] E. Gourlay, P. Glé, S. Marceau, C. Foy, S. Moscardelli, Effect of water content on the acoustical and thermal properties of hemp concretes, Constr. Build. Mater. 139 (2017) 513–523. https://doi.org/10.1016/j.conbuildmat.2016.11.018.

[101] C. Magniont, Contribution à la formulation et à la caractérisation d’un écomatériau de construction à base d’agroressources, Thèse de doctorat, Toulouse 3, 2010. https://www.theses.fr/2010TOU30101 (accessed June 23, 2020).

[102] R.L. Hamilton, O.K. Crosser, Thermal conductivity of heterogeneous two-component systems, Ind. Eng. Chem. Fundam. 1 (1962) 187–191. https://doi.org/10.1021/i160003a005.

[103] C. Boutin, Conductivité thermique du béton cellulaire autoclavé: modélisation par méthode autocohérente, Mater. Struct. 29 (1996) 609–615. https://doi.org/10.1007/BF02485968.

[104] T.H. Pham, J. Férec, V. Picandet, J. Costa, P. Pilvin, Etude expérimentale et numérique de la conductivité thermique d’un composite chaux–chanvre, (2012) 11.

[105] S.T. Nguyen, A.D. Tran-Le, M.N. Vu, Q.D. To, O. Douzane, T. Langlet, Modeling thermal conductivity of hemp insulation material: A multi-scale homogenization approach, Build. Environ. 107 (2016) 127–134. https://doi.org/10.1016/j.buildenv.2016.07.026.

[106] S. Dartois, S. Mom, H. Dumontet, A. Ben Hamida, An iterative micromechanical modeling to estimate the thermal and mechanical properties of polydisperse composites with platy particles: Application to anisotropic hemp and lime concretes, Constr. Build. Mater. 152 (2017) 661–671. https://doi.org/10.1016/j.conbuildmat.2017.06.181.

[107] S. Mom, Modèle d'homogénéisation itérative numérique pour des milieux non linéaires morphologiquement riches : application aux comportements de bétons de chanvre, Thèse de doctorat, Université Paris 6, 2013. http://www.theses.fr/2013PA066558 (accessed June 23, 2020).

[108] A. Reilly, O. Kinnane, The impact of thermal mass on building energy consumption, Appl. Energy. 198 (2017) 108–121. https://doi.org/10.1016/j.apenergy.2017.04.024.

[109] E. Latif, R. Bevan, T. Woolley, Thermal Insulation Materials for Building Applications, ICE Publishing, 2019. https://doi.org/10.1680/timfba.63518.

[110] P. de Bruijn, P. Johansson, Moisture fixation and thermal properties of lime–hemp concrete, Constr. Build. Mater. 47 (2013) 1235–1242. https://doi.org/10.1016/j.conbuildmat.2013.06.006.

[111] O. Kinnane, G. McGranaghan, R. Walker, S. Pavía, G. Byrne, A.J. Robinson, Experimental investigation of thermal inertia properties in hemp-lime concrete walls, in: Undefined, 2015. /paper/Experimental-investigation-of-thermal-inertia-in-Kinnane-McGranaghan/b3d8047eedcd8de559e1c449f609ba3bc03e13c8 (accessed June 25, 2020).

[112] A. Reilly, O. Kinnane, F.J. Lesage, G. McGranaghan, S. Pavía, R. Walker, R. O'Hegarty, A.J. Robinson, The thermal diffusivity of hemplime, and a method of direct measurement, Constr. Build. Mater. 212 (2019) 707–715. https://doi.org/10.1016/j.conbuildmat.2019.03.264.

[113] R. Walker, S. Pavía, Thermal performance of a selection of insulation materials suitable for historic buildings, Build. Environ. 94 (2015) 155–165. https://doi.org/10.1016/j.buildenv.2015.07.033.

[114] J. Kwiatkowski, M. Woloszyn, J.-J. Roux, Modelling of hysteresis influence on mass transfer in building materials, Build. Environ. 44 (2009) 633–642. https://doi.org/10.1016/j.buildenv.2008.05.006.

[115] M. Rahim, O. Douzane, A.D. Tran Le, G. Promis, T. Langlet, Characterization and comparison of hygric properties of rape straw concrete and hemp concrete, Constr. Build. Mater. 102 (2016) 679–687. https://doi.org/10.1016/j.conbuildmat.2015.11.021.

[116] F. Collet, J. Chamoin, S. Pretot, C. Lanos, Comparison of the hygric behaviour of three hemp concretes, Energy Build. 62 (2013) 294–303. https://doi.org/10.1016/j.enbuild.2013.03.010.

[117] T. Colinart, P. Glouannec, Temperature dependence of sorption isotherm of hygroscopic building materials. Part 1: Experimental evidence and modeling, Energy Build. 139 (2017) 360–370. https://doi.org/10.1016/j.enbuild.2016.12.082.

[118] Y. Aït Oumeziane, S. Moissette, M. Bart, C. Lanos, Influence of temperature on sorption process in hemp concrete, Constr. Build. Mater. 106 (2016) 600–607. https://doi.org/10.1016/j.conbuildmat.2015.12.117.

[119] A.D.T. Le, D. Samri, M. Rahim, O. Douzane, G. Promis, T. Langlet, Effect of Temperature-dependent Sorption Characteristics on The Hygrothermal Behavior of Hemp Concrete, Energy Procedia. 78 (2015) 1449–1454. https://doi.org/10.1016/j.egypro.2015.11.169.

[120] A. Evrard, A.D. Herde, Hygrothermal Performance of Lime-Hemp Wall Assemblies:, J. Build. Phys. (2009). https://doi.org/10.1177/1744259109355730.

[121] F. Collet, S. Pretot, Experimental highlight of hygrothermal phenomena in hemp concrete wall, Build. Environ. 82 (2014) 459–466. https://doi.org/10.1016/j.buildenv.2014.09.018.

[122] T. Bejat, A. Piot, A. Jay, L. Bessette, Study of Two Hemp Concrete Walls in Real Weather Conditions, Energy Procedia. 78 (2015) 1605–1610. https://doi.org/10.1016/j.egypro.2015.11.221.

[123] T. Colinart, D. Lelievre, P. Glouannec, Experimental and numerical analysis of the transient hygrothermal behavior of multilayered hemp concrete wall, Energy Build. 112 (2016) 1–11. https://doi.org/10.1016/j.enbuild.2015.11.027.
[124] U. Dhakal, U. Berardi, M. Gorgolewski, R. Richman, Hygrothermal performance of hempcrete for Ontario (Canada) buildings, J. Clean. Prod. 142 (2017) 3655–3664. https://doi.org/10.1016/j.jclepro.2016.10.102.
[125] A. Piot, T. Béjat, A. Jay, L. Bessette, E. Wurtz, L. Barnes-Davin, Study of a hempcrete wall exposed to outdoor climate: Effects of the coating, Constr. Build. Mater. 139 (2017) 540–550. https://doi.org/10.1016/j.conbuildmat.2016.12.143.
[126] C. Maalouf, C. Ingrao, F. Scrucca, T. Moussa, A. Bourdot, C. Tricase, A. Presciutti, F. Asdrubali, An energy and carbon footprint assessment upon the usage of hemp-lime concrete and recycled-PET façades for office facilities in France and Italy, J. Clean. Prod. 170 (2018) 1640–1653. https://doi.org/10.1016/j.jclepro.2016.10.111.
[127] M.M.I. Alam, Hygrothermal performance of hempcrete infill wall systems in cold climates, (2020). https://mspace.lib.umanitoba.ca/xmlui/handle/1993/34710 (accessed July 2, 2020).
[128] A.D. Tran Le, C. Maalouf, T.H. Mai, E. Wurtz, F. Collet, Transient hygrothermal behaviour of a hemp concrete building envelope, Energy Build. 42 (2010) 1797–1806. https://doi.org/10.1016/j.enbuild.2010.05.016.
[129] C. Maalouf, A.D.T. Le, S.B. Umurigirwa, M. Lachi, O. Douzane, Study of hygrothermal behaviour of a hemp concrete building envelope under summer conditions in France, Energy Build. 77 (2014) 48–57. https://doi.org/10.1016/j.enbuild.2014.03.040.
[130] B. Moujalled, Y. Aït Ouméziane, S. Moissette, M. Bart, C. Lanos, D. Samri, Experimental and numerical evaluation of the hygrothermal performance of a hemp lime concrete building: A long term case study, Build. Environ. 136 (2018) 11–27. https://doi.org/10.1016/j.buildenv.2018.03.025.
[131] G. Costantine, C. Maalouf, T. Moussa, G. Polidori, Experimental and numerical investigations of thermal performance of a Hemp Lime external building insulation, Build. Environ. 131 (2018) 140–153. https://doi.org/10.1016/j.buildenv.2017.12.037.
[132] J. Allard, N. Atalla, Propagation of Sound in Porous Media: Modelling Sound Absorbing Materials 2e, John Wiley & Sons, 2009.
[133] P.-Y. Bütschi, C. Deschenaux, B. Miao, N.K. Srivastava, Caractérisation d’une maçonnerie composée d’éléments en aggloméré de chanvre, Can. J. Civ. Eng. 31 (2004) 526–529. https://doi.org/10.1139/l04-028.
[134] P. Glé, Acoustique des Matériaux du Bâtiment à base de Fibres et Particules Végétales - Outils de Caractérisation, Modélisation et Optimisation, Thèse de doctorat, INSA de Lyon, 2013. https://tel.archives-ouvertes.fr/tel-00923665 (accessed June 23, 2020).
[135] G. Delannoy, S. Marceau, P. Glé, E. Gourlay, M. Guéguen-Minerbe, D. Diafi, I. Nour, S. Amziane, F. Farcas, Influence of binder on the multiscale properties of hemp concretes, Eur. J. Environ. Civ. Eng. 23 (2019) 609–625. https://doi.org/10.1080/19648189.2018.1457571.
[136] O. Kinnane, A. Reilly, J. Grimes, S. Pavia, R. Walker, Acoustic absorption of hemp-lime construction, Constr. Build. Mater. 122 (2016) 674–682. https://doi.org/10.1016/j.conbuildmat.2016.06.106.
[137] P. Glé, E. Gourdon, L. Arnaud, Modelling of the acoustical properties of hemp particles, Constr. Build. Mater. 37 (2012) 801–811. https://doi.org/10.1016/j.conbuildmat.2012.06.008.
[138] M. Degrave-Lemeurs, P. Glé, A. Hellouin de Menibus, Acoustical properties of hemp concretes for buildings thermal insulation: Application to clay and lime binders, Constr. Build. Mater. 160 (2018) 462–474. https://doi.org/10.1016/j.conbuildmat.2017.11.064.
[139] R. Fernea, D.L. Manea, L. Plesa, R. Iernuțan, M. Dumitran, Acoustic and thermal properties of hemp-cement building materials, Procedia Manuf. 32 (2019) 208–215. https://doi.org/10.1016/j.promfg.2019.02.204.

[140] M.P. Boutin, C. Flamin, S. Quinton, G. Gosse, Etude des caractéristiques environnementales du chanvre par l'analyse de son cycle de vie, (2006).
[141] Building regulations approval, GOV.UK. (2010). https://www.gov.uk/building-regulations-approval (accessed July 1, 2020).
[142] A. Laukaitis, B. Fiks, Acoustical properties of aerated autoclaved concrete, Appl. Acoust. 67 (2006) 284–296. https://doi.org/10.1016/j.apacoust.2005.07.003.
[143] L. Zampori, G. Dotelli, V. Vernelli, Life Cycle Assessment of Hemp Cultivation and Use of Hemp-Based Thermal Insulator Materials in Buildings, Environ. Sci. Technol. 47 (2013) 7413–7420. https://doi.org/10.1021/es401326a.
[144] H.M.G. van der Werf, Life Cycle Analysis of field production of fibre hemp, the effect of production practices on environmental impacts, Euphytica. 140 (2004) 13–23. https://doi.org/10.1007/s10681-004-4750-2.
[145] B. Sodagar, D. Rai, B. Jones, J. Wihan, R. Fieldson, The carbon-reduction potential of straw-bale housing, Build. Res. Inf. 39 (2011) 51–65. https://doi.org/10.1080/09613218.2010.528187.
[146] A. Arrigoni, R. Pelosato, P. Melià, G. Ruggieri, S. Sabbadini, G. Dotelli, Life cycle assessment of natural building materials: the role of carbonation, mixture components and transport in the environmental impacts of hempcrete blocks, J. Clean. Prod. 149 (2017) 1051–1061. https://doi.org/10.1016/j.jclepro.2017.02.161.
[147] B. Berge, The Ecology of Building Materials, Routledge, 2009.
[148] Defra, Planting and growing Miscanthus best practice guidelines, (2007).
[149] T. Nakajima, T. Yamada, K.G. Anzoua, R. Kokubo, K. Noborio, Carbon sequestration and yield performances of Miscanthus × giganteus and Miscanthus sinensis, Carbon Manag. 9 (2018) 415–423. https://doi.org/10.1080/17583004.2018.1518106.
[150] G.D. Price, K. Winkle, W.R. Gehrels, A geochemical record of the mining history of the Erme Estuary, south Devon, UK, Mar. Pollut. Bull. 50 (2005) 1706–1712. https://doi.org/10.1016/j.marpolbul.2005.07.016.
[151] K. Tatsi, A. Turner, Distributions and concentrations of thallium in surface waters of a region impacted by historical metal mining (Cornwall, UK), Sci. Total Environ. 473–474 (2014) 139–146. https://doi.org/10.1016/j.scitotenv.2013.12.003.
[152] D.R.S. Middleton, M.J. Watts, D.J. Beriro, E.M. Hamilton, G.S. Leonardi, T. Fletcher, R.M. Close, D.A. Polya, Arsenic in residential soil and household dust in Cornwall, south west England: potential human exposure and the influence of historical mining, Environ. Sci. Process. Impacts. 19 (2017) 517–527. https://doi.org/10.1039/C6EM00690F.
[153] J. Figala, V. Vranová, K. Rejšek, P. Formánek, Giant miscanthus (Miscantus × Giganteus Greef Et Deu.) – A Promising Plant for Soil Remediation: A Mini Review, Acta Univ. Agric. Silvic. Mendel. Brun. 63 (2015) 2241–2246.
[154] G. Dražić, J. Milovanović, S. Stefanović, I. Petrić, Potential of miscanthus × giganteus for heavy metals removing from industrial deposol, Acta Reg. Environ. 14 (2017) 56–58. https://doi.org/10.1515/aree-2017-0009.
[155] N. Wanat, Potential adaptation of Miscanthus x giganteus for the phytoremediation of a former mine site highly contaminated, Ph.D. Thesis, Université de Limoges, 2011. https://tel.archives-ouvertes.fr/tel-00809037 (accessed June 23, 2020).
[156] W. Brostow, T. Datashvili, P. Jiang, H. Miller, Recycled HDPE reinforced with sol–gel silica modified wood sawdust, Eur. Polym. J. 76 (2016) 28–39. https://doi.org/10.1016/j.eurpolymj.2016.01.015.
[157] R. Jeencham, N. Suppakarn, K. Jarukumjorn, Effect of flame retardants on flame retardant, mechanical, and thermal properties of sisal fiber/polypropylene composites, Compos. Part B Eng. 56 (2014) 249–253. https://doi.org/10.1016/j.compositesb.2013.08.012.

[158] N. Saba, M.T. Paridah, K. Abdan, N.A. Ibrahim, Effect of oil palm nano filler on mechanical and morphological properties of kenaf reinforced epoxy composites, Constr. Build. Mater. 123 (2016) 15–26. https://doi.org/10.1016/j.conbuildmat.2016.06.131.

[159] A. Schirp, S. Su, Effectiveness of pre-treated wood particles and halogen-free flame retardants used in wood-plastic composites, Polym. Degrad. Stab. 126 (2016) 81–92. https://doi.org/10.1016/j.polymdegradstab.2016.01.016.

[160] H.A. Khalil, M. Tehrani, Y. Davoudpour, A. Bhat, M. Jawaid, A. Hassan, Natural fiber reinforced poly(vinyl chloride) composites: A review, J. Reinf. Plast. Compos. 32 (2013) 330–356. https://doi.org/10.1177/0731684412458553.

[161] H.M. Akil, C. Santulli, F. Sarasini, J. Tirillò, T. Valente, Environmental effects on the mechanical behaviour of pultruded jute/glass fibre-reinforced polyester hybrid composites, Compos. Sci. Technol. 94 (2014) 62–70. https://doi.org/10.1016/j.compscitech.2014.01.017.

[162] C. Suresh Kumar, V. Arumugam, H.N. Dhakal, R. John, Effect of temperature and hybridisation on the low velocity impact behavior of hemp-basalt/epoxy composites, Compos. Struct. 125 (2015) 407–416. https://doi.org/10.1016/j.compstruct.2015.01.037.

[163] M. Asim, N. Saba, M. Jawaid, M. Nasir, M. Pervaiz, O.Y. Alothman, A Review on Phenolic Resin and its Composites, (2017). https://doi.org/10.2174/1573411013666171003154410.

[164] M.H. Gheith, M.A. Aziz, W. Ghori, N. Saba, M. Asim, M. Jawaid, O.Y. Alothman, Flexural, thermal and dynamic mechanical properties of date palm fibres reinforced epoxy composites, J. Mater. Res. Technol. 8 (2019) 853–860. https://doi.org/10.1016/j.jmrt.2018.06.013.

[165] N. Saba, M.T. Paridah, M. Jawaid, Mechanical properties of kenaf fibre reinforced polymer composite: A review, Constr. Build. Mater. 76 (2015) 87–96. https://doi.org/10.1016/j.conbuildmat.2014.11.043.

[166] N. Saba, M. Jawaid, M.T. Paridah, O.Y. Al-othman, A review on flammability of epoxy polymer, cellulosic and non-cellulosic fiber reinforced epoxy composites, Polym. Adv. Technol. 27 (2016) 577–590. https://doi.org/10.1002/pat.3739.

[167] M. Asim, M. Jawaid, A. Khan, A.M. Asiri, M.A. Malik, Effects of Date Palm fibres loading on mechanical, and thermal properties of Date Palm reinforced phenolic composites, J. Mater. Res. Technol. 9 (2020) 3614–3621. https://doi.org/10.1016/j.jmrt.2020.01.099.

[168] A. Khan, R. Vijay, D. Lenin Singaravelu, G.R. Arpitha, M.R. Sanjay, S. Siengchin, M. Jawaid, K. Alamry, A.M. Asiri, Extraction and characterization of vetiver grass (Chrysopogon zizanioides) and kenaf fiber (Hibiscus cannabinus) as reinforcement materials for epoxy based composite structures, J. Mater. Res. Technol. 9 (2020) 773–778. https://doi.org/10.1016/j.jmrt.2019.11.017.

[169] F. Hanan, M. Jawaid, P. Md Tahir, Mechanical performance of oil palm/kenaf fiber-reinforced epoxy-based bilayer hybrid composites, J. Nat. Fibers. 17 (2020) 155–167. https://doi.org/10.1080/15440478.2018.1477083.

[170] S. M.r., S. Siengchin, J. Parameswaranpillai, M. Jawaid, C.I. Pruncu, A. Khan, A comprehensive review of techniques for natural fibers as reinforcement in composites: Preparation, processing and characterization, Carbohydr. Polym. 207 (2019) 108–121. https://doi.org/10.1016/j.carbpol.2018.11.083.

[171] K.L. Pickering, M.G.A. Efendy, T.M. Le, A review of recent developments in natural fibre composites and their mechanical performance, Compos. Part Appl. Sci. Manuf. 83 (2016) 98–112. https://doi.org/10.1016/j.compositesa.2015.08.038.

[172] O. Onuaguluchi, N. Banthia, Plant-based natural fibre reinforced cement composites: A review, Cem. Concr. Compos. 68 (2016) 96–108. https://doi.org/10.1016/j.cemconcomp.2016.02.014.

[173] E. Boix, F. Georgi, P. Navard, Influence of alkali and Si-based treatments on the physical and chemical characteristics of miscanthus stem fragments, Ind. Crops Prod. 91 (2016) 6–14. https://doi.org/10.1016/j.indcrop.2016.06.030.
[174] E. Boix, E. Gineau, J.O. Narciso, H. Höfte, G. Mouille, P. Navard, Influence of chemical treatments of miscanthus stem fragments on polysaccharide release in the presence of cement and on the mechanical properties of bio-based concrete materials, Cem. Concr. Compos. 105 (2020) 103429. https://doi.org/10.1016/j.cemconcomp.2019.103429.
[175] Y. Lv, G. Ye, G. De Schutter, Utilization of miscanthus combustion ash as internal curing agent in cement-based materials: Effect on autogenous shrinkage, Constr. Build. Mater. 207 (2019) 585–591. https://doi.org/10.1016/j.conbuildmat.2019.02.167.

Table 1. Chemical composition of bio-based aggregates (hemp and miscanthus)

Species	Genotype	Lignin	Cellulose	Hemicellulose	H:L*	Ash
Hemp (cannabis sativa)						
Vignon et al. [22]	n/a	28.00	44.00	18.00	2.21	2.00
Thomsen et al. [23]	n/a	17-19	48.00	21-25	3.90	n/a
Sedan [8]	n/a	6.00	56.10	10.90	11.17	n/a
Diquelou et al. [24]	n/a	21.80	47.30	18.30	3.01	3.70
Viel et al. [25]	n/a	9.52	49.97	21.42	7.50	0.67
Mean		**16.33**	**49.34**	**17.16**	**5.97**	**2.12**
SD**		8.93	4.00	3.85	3.34	1.24
Miscanthus (Hodgson et al. [26]**)**						
M. x Giganteus	EM101	12.02	50.34	24.83	6.25	2.67
M. sacchariflorus	EM105	12.1	49.06	27.41	6.32	2.29
M. Sinensis (hybrid)	EM108	9.27	43.06	33.14	8.22	3.47
M. sinensis	EM111	9.69	43.18	33.98	7.96	3.19
M. sinensis	EM115	9.23	47.59	33.00	8.73	2.44
Mean		**10.46**	**46.65**	**30.47**	**7.50**	**2.81**
SD**		1.47	3.36	4.09	1.14	0.52

*H:L Cellulose + Hemicellulose / lignin ratio and ** SD standard deviation

Table 1. Infra-red vibration bands and associated chemical components [27]

wavenumber (cm^{-1})	**Vibration bonds**	**Chemicals**

3336	OH stretching	Cellulose, Hemicellulose
2887	C-H symmetrical stretching	Cellulose, Hemicellulose
1729	C=O stretching vibration	Pectin, waxes
1623	O-H bending of absorbed water	Water
1506	C=C aromatic symmetrical stretching	Lignin
1423	HCH and OCH in-plane bending vibration	Cellulose
1368, 1362	In-plane C-H bending	Cellulose, Hemicellulose
1317	CH2 rocking vibration	Cellulose
1246	C=O and G ring stretching	Lignin
1202	C-O-C symmetric stretching	Cellulose, Hemicellulose
1155	C-O-C asymmetrical stretching	Cellulose, Hemicellulose
1048, 1019, 995	C-C, C-OH, C-H ring and side group vibrations	Cellulose, Hemicellulose
896	COC, CCO and CCH deformation and stretching	Cellulose
662	C-OH out of plane bending	Cellulose

Table 2. Physical properties (densities and porosities) of hemps hurds and miscanthus particles.

References - indications	ρ_b(kg/m^3)	ρ_p(kg/m^3)	ρ_s(kg/m^3)	Φ_{inter}(%)	Φ_{intra}(%)	Φ_T (%)
Hemp shiv particles						
Cérézo, 2005 [6]	130.0	320.0	1455	59.4	31.8	78.0
Nguyen, 2010 [10] - Un-fibered	102.8	256.5	1465	59.9	33.1	93.0
Nguyen, 2010 [10] - Fibered	54.9	256.4	1438	78.6	17.6	96.2
Nozahic, 2014 [7]	114.2	256.0	1540	55.1	37.2	92.4
Chamoin, 2013 [9]	110.0	250.0	1348	56.0	36.1	92.1
Mazhoud, 2017 [33]	107.4	256.4	1376	58.1	34.1	92.2
Miscanthus aggregates						
Chen et al., 2017 [32] - 0-2 mm	77.60	222.20	1406	65.1/**65.1**	58.1/**29**	**94.5**
Chen et al., 2017 [32] - 2-4 mm	119.4	250.0	1400	52.2/**52.2**	38.3/**39**	**91.5**

Table 3. Constituent ratios, production and curing methodologies for bio-based building materials (hemp) (Adapted from Hirst [67]). (+) T70 is a commercial binder with 37% hydraulic lime, 63% calcic lime; Tradichanvre is a commercial plastering lime made of 22% hydraulic lime, 58% calcic lime and 20% fine sand. (++) Tradical PF70 is made of 75% calcic lime CL90s, 15% hydraulic binder, 10% pozzolanic binder and ~0.5% of additives; Tradichanvre is made of 65% of Tradical PF70 and 35% of sand ($CaCO_3$). (*) A detailed account of composition of binder blends used in bio-based building materials is shown in Table 5.

Binder type (*)	A (kg)	B(kg)	W(l)	Mixing regime	Specimen dimensions	Fabrication and demoulding regime	Curing regime
(Cérézo) [6]							
T70 and Tradichanvre(+)	1	1.73	3.05	Mix dry hemp for 2 minutes, add and mix with the pre-wetting water for 5 minutes, add the binder and mix for 2 minutes, add the binder water and mix for 5 minutes. Total mixing time: 14 minutes	Φ 160 x 320 mm^3 waxed carbonated moulds for compression testing	Tamped in 80mm layers at 0.05MPa (1kN over 200cm^2). Kept in moulds until testing date. Stored horizontally with all faces exposed.	Kept at 20°C and 50% relative humidity until testing dates at 21 days, 3, 6, 9, 12, 15, 18, and 24 months.
	1	2.59	3.36				
	1	1.81	3.11				
	1	2.41	3.35				
	1	3.61	3.82				
	1	4.82	4.29				
(Construire en Chanvre) [62]							
A mix of Lime, quick setting cement and OPC recommended	1	1	2	Drum mixer (slow mixing rate, maximum tilt) – mix water and binder to slurry, add hemp until homogeneous. Pan mixer (slowest rate of rotation) –mix hemp and 1/3 of water. Progressively add binder and rest of water until homogeneous.	n/a	n/a	n/a
	1	2.2	3.5				
	1	2.7	5				
	1	5	5				
(Evrard) [11]							
Trdical PF70 and Tradichanvre (++)	1	2	3	No mixing details. Total mixing time of ~ 4 minutes	Φ 190 x 35 mm^3	Loose-drop into moulds and surface level with hand. Demould 3 to 5 days after casting.	Kept at 20°C and 100% relative humidity for 3 to 5 days, then at 23°C ; 65% relative humidity for 1 month
	1	1	2				
	1	6	4				

Error! Not a valid result for table.. Continued

References & sample ID	A (kg)	B(kg)	W(l)	Mixing regime	Specimen dimensions	Fabrication and demoulding regime	Curing regime
(Strandberg, P.) [68]							
NHL5, CEMII/A-L and calcined gypsum (beta-hemihydrate)	1.0	3.57	3.78	Mix binder and water to slurry, add hemp and then add additional water to achieve desired consistency. Remove to cast five minutes after all constituents have been added.	150x150x150mm^3 steel moulds for compression tests. Φ 150 x 300mm steel moulds for splitting tests.	Tamped in 50mm layers with a 45x45mm wooden stave. Then subjected to 50Hz vibrating table for 1 minute. De-moulded after 2 days.	Phase 1 – cured for 12 weeks at 20°C then in carbonation room for 40 days. Testing at 18 weeks. Phase 2 – stored in carbonation room for 40 days immediately after de-moulding. Testing at 12 weeks. Carbonation room: 4.5% CO_2 at 20°C and 50%rh at 40th day CO_2 levels reduced to 0.038% until testing.
	1.0	3.03	4.03				
	1.0	3.33	4.00				
	1.0	3.57	3.96				
	1.0	4.55	4.05				
	1.0	4.55	6.68				
(Nguyen) [10]							
Tradical PF70, NHL2, NHL3.5 Z and CEMI 52.5 N	1.0	1.11	0.6	Aggregate introduction and mixing for 2 minutes, pre-wetting water addition and mixing for 5 min, binder addition and mixing for 2 min, the addition of mixing water and mixing for 5 minutes.	Φ 100 x 200 mm height	Samples compacted (0.07MPa -2.08 MPa) kept in moulds and demoulded 48 hours later. Curing at 20±2°C and 75±5% rh	20°C ± 2°C; 75% RH ± 15% until testing at 28 and 180 days.
	1.0	2.15	1.42				
	1.0	2.15	1.18				
	1.0	2.15	1.99				
	1.0	3.84	3.57				
(Williams) [66]							
Trdical PF70	1.0	2.2	3	Binder and water mixed for 3 min with an initial hand mixing of 01 min and shiv added to the slurry and mixed for another 2 min	400x150x150 mm^3 prisms for strength testing, 400x400x50 mm^3 prisms for thermal conductivity	Samples were compacted at 30%,45% and 60% into weighted layers of 25mm, 50mm and 150 mm and kept at ISC conditions at 20°C and 50%rh and demoulded after 06 days	Indoor Standard Conditions at 20°C and 50%rh
	1.0	1.8	3				
	1.0	2.2	3				
	1.0	2.6	3				
	1.0	2.2	3				

A: aggregate mass, B: Binder mass, W: Water volume (A,B and W in a cubic metre of composite), Φ : diameter, n/a: not available, OPC: Ordinary Portland Cement

Table 4. The composition of pre-formulated binders presented by different studies (weight percentages). Adapted from Williams [66].

References	**Binder**	**Binder composition**				
		Hydrated lime	**Hydraulic lime**	**Cement**	**Pozzolans**	**Others**
Elfordy et al. [69], Nguyen et al. [70], Nguyen [10], Kioy [71],Kashtanjeva et al.[72], Tronet et al.[64,73], Youssef et al. [74]	Tradical PF70	70-75	15	0	10-15	0-0.5 (additives)
Cérézo [6], Evrard [11], Collet et al.[75]	Tradicanvre	55-58	10-22	0	0	20-35 (Sand)
	Batichanvre	70	30	0	0	0
Hirst et al. [76], Hirst [67]	Tradical HB	50-80	10-70	0	5-10	0
Walker et al. [77], Pavia et al. [78], Stevulova et al.[79],	Cement blend	50-70	0-20	10-50	0	0
Walker et al. [77], Magniont et al. [80] , Pavia and Walker [81], Sinka et al.[82], Dinh [41]	Metakaolin blend	30-80	0	0	20-70 (MK)	0
Walker et al. [77], Pavia and Walker [81]	GGBS	70	0	0	30(GGBS)	0
Nozahic et al. [63], Amziane et al. [83]	Pumice blend	10-19	0	0	77-90	0-4 (Na_2SO_4)
Balčiūnas et al.[84]	Clay blend	33	0	33	0	33(clay)

(GGBS): Ground granulated blast furnace slag, (MK): Metakaolin

Table 6. Mechanical properties of manually tamped hemp - lime composites.

Reference	Binder vol. ratio	ρ (kg/m^3)	σ_{max}(N/mm^2)	E(N/mm^2)	$\varepsilon_{(\sigma max)}$	υ (Poisson)
Cérézo [6]	10%	250	0.25	4.00	0.15	0.05
	19-29%	350-500	0.35-0.80	32-95	0.05-0.06	0.08-0.16
	40%	600-660	1.15	140-160	0.04	0.20

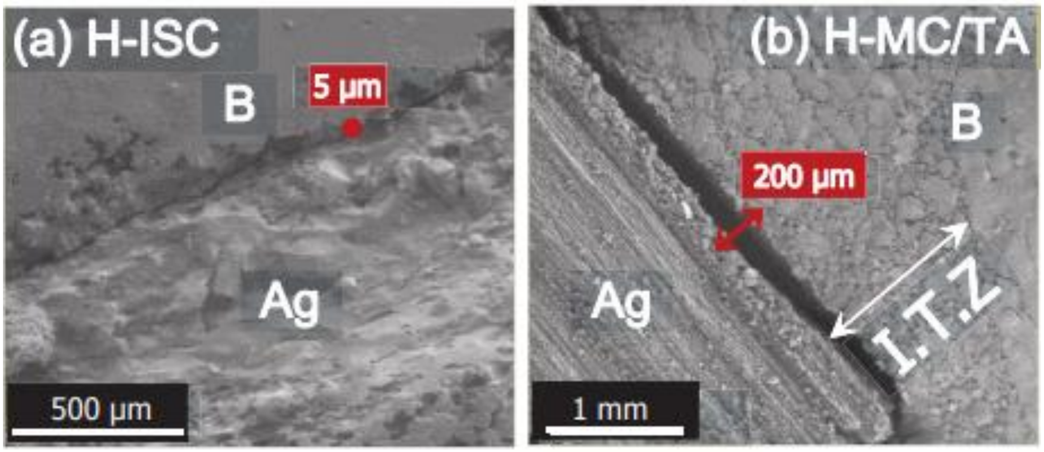

Figure 1. Lime–aggregate interfaces by SEM on pellets cured 14 days. (a) indoor standard curing and (20°C and 50%rh), (c) moist curing (20°C and 95%rh) and thermal activation (50°C and 95%rh) Ag: Aggregate, B: Binder and ITZ: Interfacial transitional zone [28].

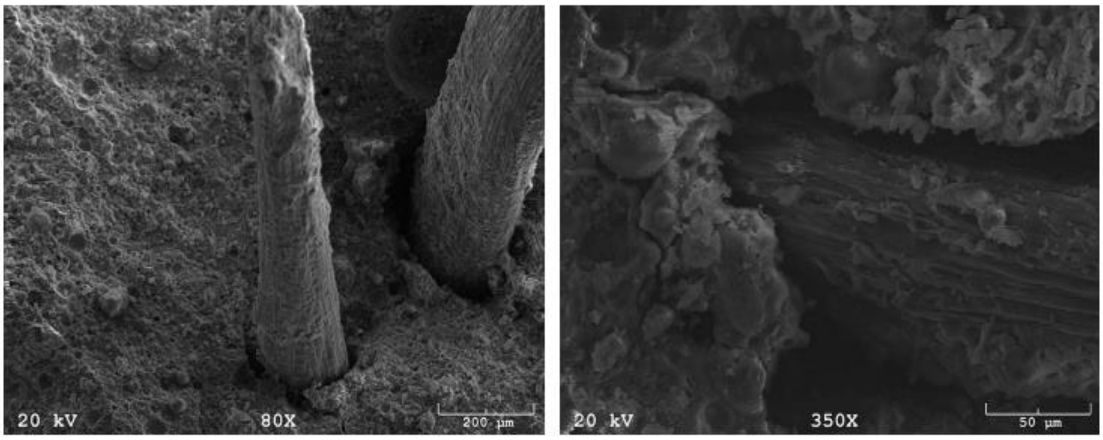

Figure 2. SEM micrographs at 80x (left) and 350x (light) of the coir / coconut fibre - geopolymer matrix interface [55].

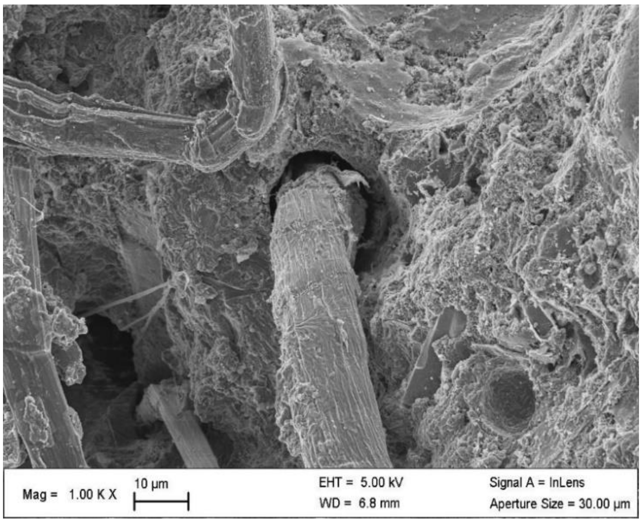

Figure 3. SEM micrograph of the interface between a flax fibre and a cementitious matrix [56].

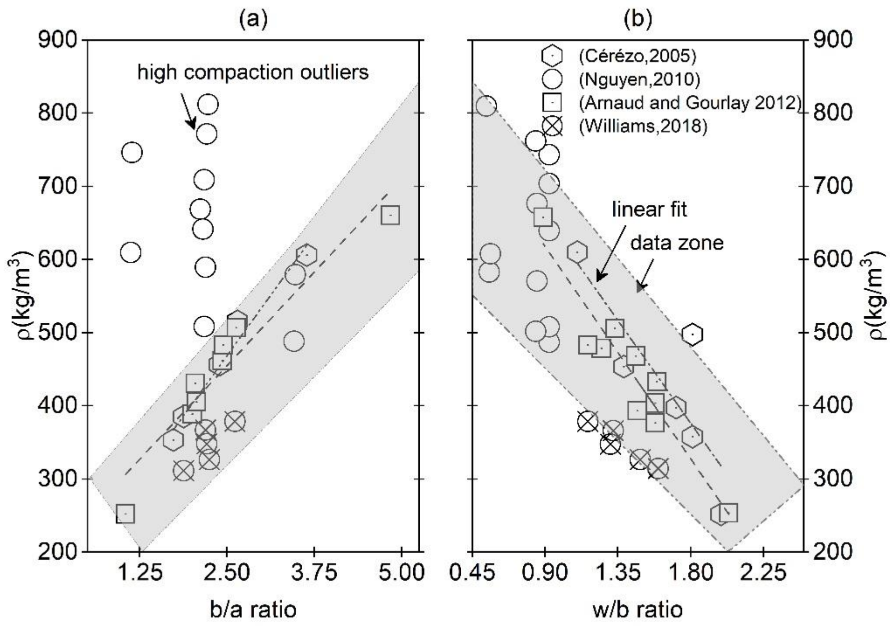

Figure 4. The evolution of final unit weight of hemp concretes: (a) as a function of binder / aggregate weight ratio (b/a ratio) and (b) water/ binder ratio (w/b ratio).

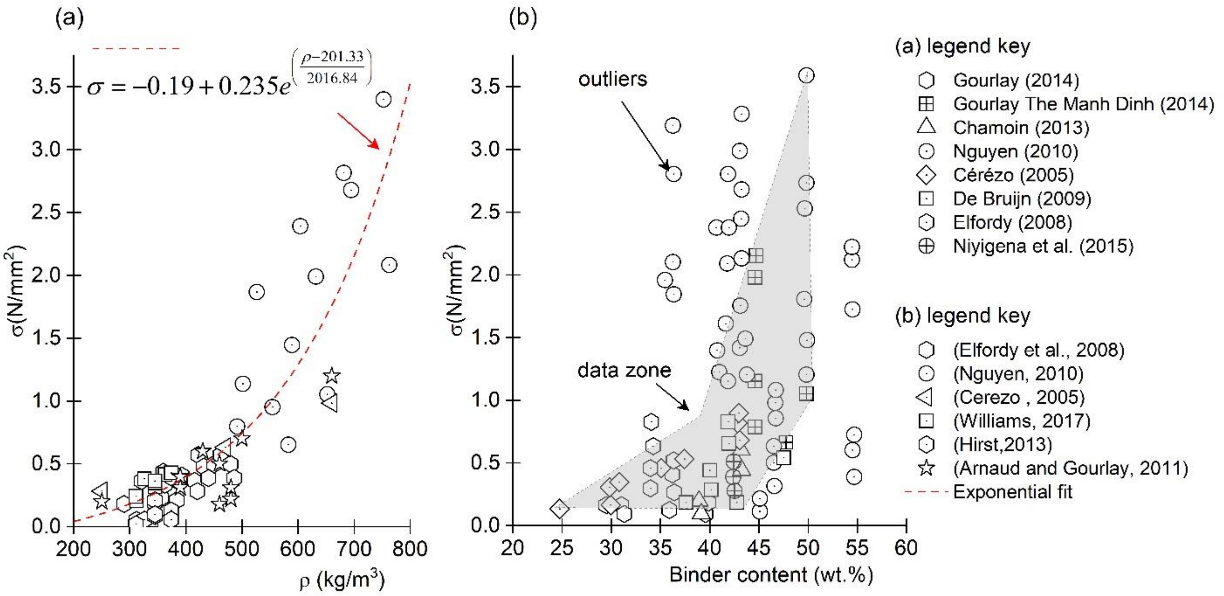

Figure 5. (a) The evolution of compressive strength as a function of unit weight (density) and (b) the strength as a function of binder content of hemp-lime reported in literature.

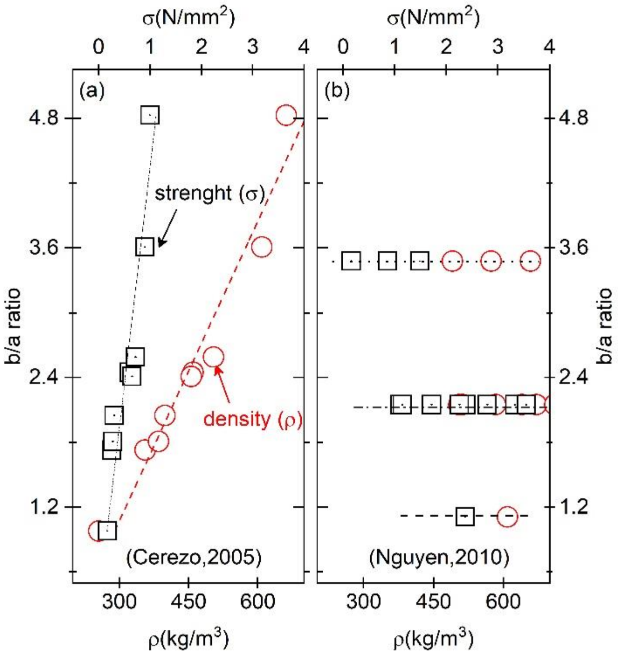

Figure 6. The evolution of unit weight and compressive strength as a function of binder to aggregate ratio for un-compacted samples (a) versus compacted samples (b).

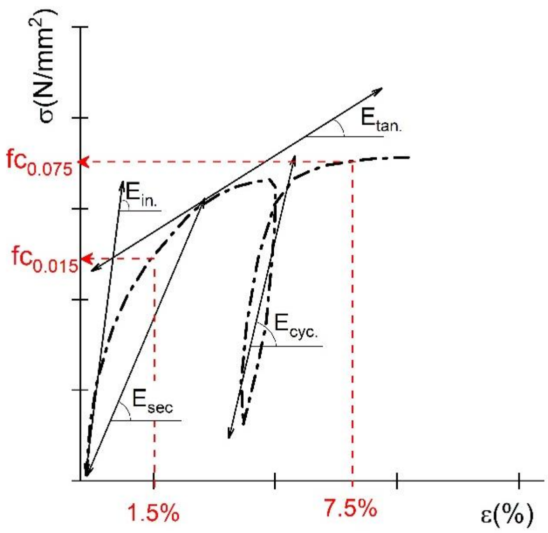

Figure 7. Stress – strain behaviour of hemp concrete and benchmarked strains at 1.5 – 7.5% [10] and different methods to determine the stiffness modulus [85]. Ein. is initial module, Esec. the secant module, Etan. the tangential module and Ecycl. the cyclic module at the 2nd phase of loading.

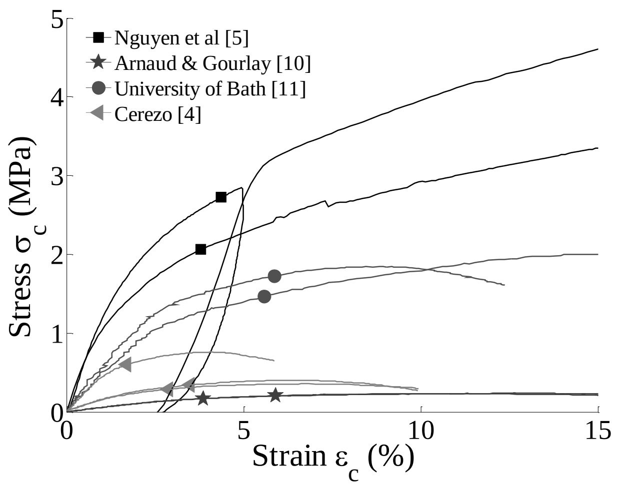

Figure 8. The different stress - strain curves of LHC taken from literature: lightly compacted LHC [10; 4; 11] behave as lightweight concretes, with a stress softening and densest LHC [5] having a large hardening area. Adapted from [73].

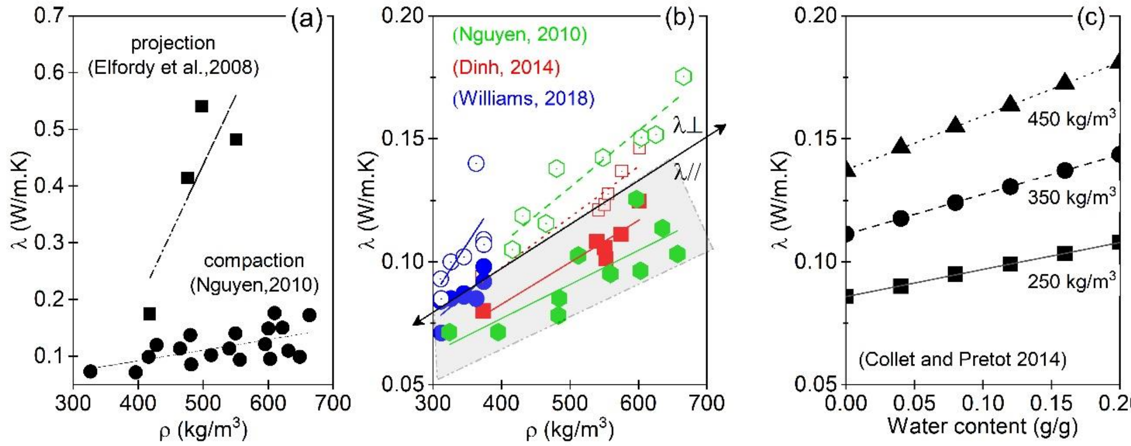

Figure 9. The evolution of thermal conductivity as a function of dry unit weight of hemp concrete and manufacturing techniques for projected and compacted hemp concrete.

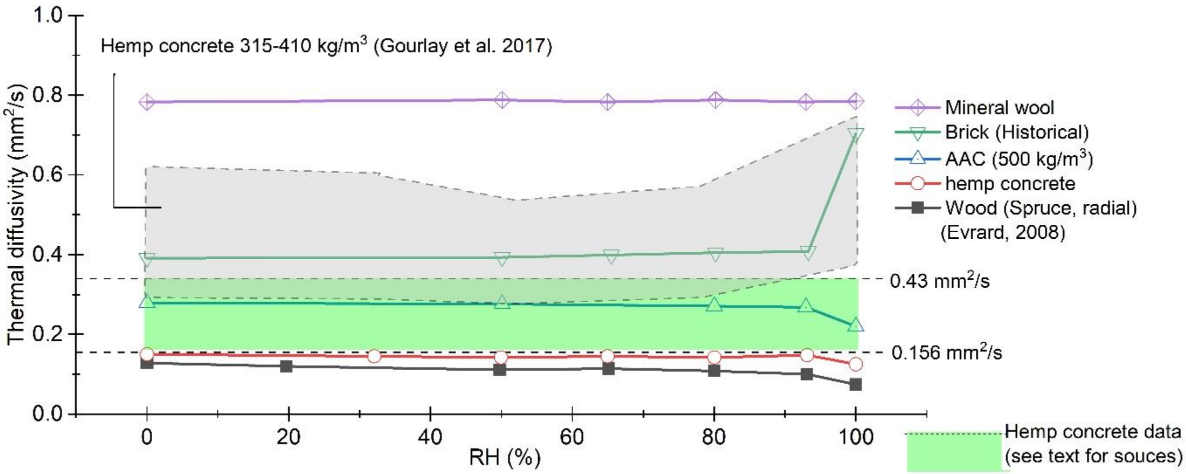

Fig. 10. Thermal diffusivity of hemp-lime concrete compared to standard wall construction materials (Mineral wool of 0.04 W/mK, Brick, aerated autoclaved concrete AAC – 500kg/m^3 and spruce wood). Adapted from [11].

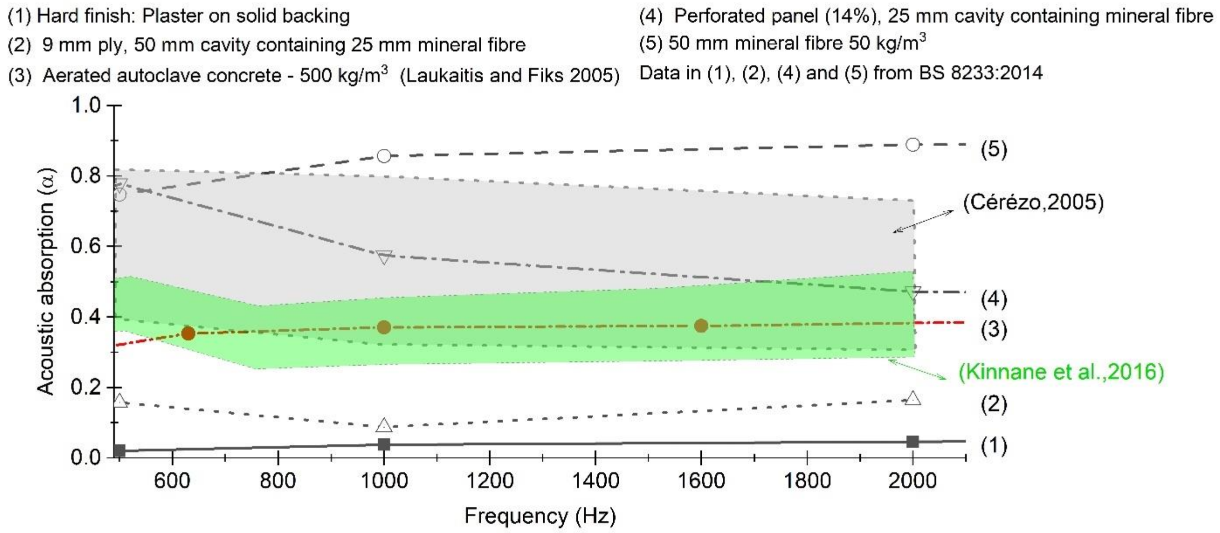

Fig. 11. Comparative analysis of acoustic absorption per octave of building materials and systems.